UIC

The University of Illinois at Chicago

Department of Mechanical Engineering

REPORT DOCUMENTATION PAGE

Form Approved
OMB NO. 0704-0188

1. AGENCY USE ONLY *(Leave blank)*	2. REPORT DATE	3. REPORT TYPE AND DATES COVERED
		Technical Report

4. TITLE AND SUBTITLE

Defiition of the Elastic Forces in the Finite Element Formulations

5. FUNDING NUMBERS

DAAG55-97-1-0303

6. AUTHOR(S)

Marcello Berzeri, Marcello Campanelli, Ahmed A. Shabana

7. PERFORMING ORGANIZATION NAMES(S) AND ADDRESS(ES)

University of Illinois at Chicago
Chicago, IL 60612

8. PERFORMING ORGANIZATION REPORT NUMBER

9. SPONSORING / MONITORING AGENCY NAME(S) AND ADDRESS(ES)

U.S. Army Research Office
P.O. Box 12211
Research Triangle Park, NC 27709-2211

10. SPONSORING / MONITORING AGENCY REPORT NUMBER

ARO 35711.13-EG

11. SUPPLEMENTARY NOTES

The views, opinions and/or findings contained in this report are those of the author(s) and should not be construed as an official Department of the Army position, policy or decision, unless so designated by other documentation.

12a. DISTRIBUTION / AVAILABILITY STATEMENT

Approved for public release; distribution unlimited.

12 b. DISTRIBUTION CODE

13. ABSTRACT *(Maximum 200 words)*

ABSTRACT IN TECHNICAL REPORT

14. SUBJECT TERMS	15. NUMBER IF PAGES
	16. PRICE CODE

17. SECURITY CLASSIFICATION OR REPORT	18. SECURITY CLASSIFICATION OF THIS PAGE	19. SECURITY CLASSIFICATION OF ABSTRACT	20. LIMITATION OF ABSTRACT

Technical Report # MBS98-1-UIC
Department of Mechanical Engineering
University of Illinois at Chicago

November 1998

DEFINITION OF THE ELASTIC FORCES

IN THE FINITE ELEMENT FORMULATIONS

Marcello Berzeri
Marcello Campanelli
Ahmed A. Shabana
Department of Mechanical Engineering
University of Illinois at Chicago
842 West Taylor Street
Chicago, IL 60607-7022

This research was supported by the U.S. Army Research Office, Research Triangle Park, NC

ABSTRACT

The equivalence of the finite element formulations used in flexible multibody dynamics is the focus of this investigation. This equivalence will be used to address several fundamental issues related to the deformations, flexible body coordinate systems, and the geometric centrifugal stiffening effect. Two conceptually different finite element formulations that lead to exact modeling of the rigid body dynamics will be used in this investigation. The first one is the absolute nodal coordinate formulation, in which beams and plates can be treated as isoparametric elements. This formulation leads to a constant and symmetric mass matrix and highly nonlinear elastic forces. It is demonstrated in this study that different element coordinate systems which are used for the convenience of describing the element deformations lead to similar results as the element size is reduced. In particular, two element frames are used in this study; the *pinned* and the *tangent frames.* The pinned frame has one of its axes passes through two nodes of the element, while the tangent frame is rigidly attached to one of the ends of the element. Numerical results obtained in this investigation using these two different frames are found to be in a good agreement as the element size decreases. The relationship between the coordinates used in the absolute nodal coordinate formulation and the floating frame of reference formulation is presented. This relationship is used to obtain the highly nonlinear expression of the strain energy used in the absolute nodal coordinate formulation from the simple energy expression used in the floating frame of reference formulation. It is shown in this paper that the source of the nonlinearity is due to the finite rotation of the element. The result of the analysis presented in this paper clearly demonstrates that the instability observed in high speed rotor analytical models due to the neglect of the geometric centrifugal stiffening is not a problem inherent to a particular finite element formulation. Such a problem can only be avoided by considering the known linear effect of the geometric centrifugal stiffening or by using a nonlinear elastic model as recently demonstrated. Fourier analysis of the solutions obtained in this investigation also sheds new light on the fundamental problem of the choice of the deformable body coordinate system in the floating frame of reference formulation.

1 INTRODUCTION

The floating frame of reference formulation is widely used in flexible multibody simulations. In this formulation, a coordinate system is assigned to each flexible body in the multibody system [13, 18]. The location and orientation of this body coordinate system are defined using absolute Cartesian and orientation coordinates. The deformation of the body with respect to its coordinate system is defined using local coordinates that can be introduced using the finite element method. The floating frame of reference formulation leads to a simple expression for the elastic forces and a highly nonlinear expression for the inertia forces. The simplicity of the elastic forces is due to the fact that the deformations of the bodies are defined with respect to their respective coordinate systems. The nonlinearity of the inertia forces is also the result of using local coordinates to describe the locations of the points on the deformable body. In order to define the absolute position, velocity and acceleration equations in the floating frame of reference formulation, a coordinate transformation that defines the orientation of the body coordinate systems with respect to a selected inertial frame is used. The use of this coordinate transformation leads to the nonlinearity and to a strong dynamic coupling between the absolute reference and the local coordinates. While the finite element floating frame of reference formulation can lead to exact modeling of the rigid body dynamics when beam elements are used, this formulation has been only used in the analysis of small deformation problems since it employes non-isoparametric beam elements.

Another conceptually different formulation which is introduced recently for the large rotation and deformation analysis [2, 3, 10, 15, 19] is the absolute nodal coordinate formulation [8, 18]. In this formulation, only absolute position and slope coordinates are used. Unlike the floating frame of reference formulation, the absolute nodal coordinate formulation leads to a simple expression for the inertia forces and a highly nonlinear expression for the elastic forces. The mass matrix is constant and symmetric, and the vector of centrifugal and Coriolis forces is identically equal to zero. In the absolute nodal coordinate formulation, exact

modeling of the rigid body dynamics can be obtained, and beams and plates can be treated as isoparametric elements. Furthermore, the formulation of joint constraints and forces can be much simpler in the absolute nodal coordinate formulation as compared to the floating frame of reference formulation [8].

It was recently demonstrated that the highly nonlinear inertia forces obtained in the floating frame of reference formulation are equivalent to the simple inertia forces obtained using the absolute nodal coordinate formulation [17]. The result of this study clearly demonstrated that the floating frame of reference formulation does not lead to a separation between the rigid body motion and the elastic deformation. A procedure for evaluating the inertia shape integrals required to evaluate the nonlinear inertia forces of the floating frame of reference formulation from the constant mass matrix of the absolute nodal coordinate formulation was presented [17].

It was observed, in high speed rotor-craft applications, that the solutions obtained using the floating frame of reference formulation incorrectly exhibit instability problems when the angular velocity of the flexible body exceeds a certain limit [11, 14]. This incorrect solution was attributed to the neglect of the centrifugal geometric stiffening effect. Studies which include the geometric stiffening effect or employ a nonlinear elastic model showed that the instability problem can be solved [7]. There has been an argument, however, that the instability problem is an inherent problem of the floating frame of reference formulation and can be avoided using a full finite element representation; and in such a full finite element representation, a correct stable solution can be obtained without the need to explicitly account for the geometric centrifugal stiffening effect nor the elastic nonlinearity. The analysis presented in this paper will be used to demonstrate that this is not the case. To this end, the absolute nodal coordinate formulation which employs a full finite element representation is used. Using the absolute nodal coordinate formulation, it will be demonstrated that the generalized elastic forces obtained using the full finite element representation are equiva-

lent to the elastic forces obtained using the floating frame of reference formulation, thereby demonstrating that the instability problem resulting from the neglect of the geometric centrifugal stiffening effect is not a problem inherent to only the floating frame of reference formulation. The results of the analysis presented in this paper, with the results previously reported [17] demonstrate that the forces used in the floating frame of reference formulation can be obtained from the forces resulting from the use of a full finite element representation by simply using coordinate transformation, provided that no linearization of the kinematic equations is employed.

This paper is organized as follows. In Section 2, a brief review of the absolute nodal coordinate formulation is presented. In Section 3 and 4, two coordinate systems, the pinned and tangent frames, shown in Fig. 1, are used to define the element deformations and the elastic forces in the absolute nodal coordinate formulation. In Section 5, it is shown that the results obtained using these two frames are in a good agreement as the element size decreases. In Section 6 and 7, the floating frame of reference formulation is briefly discussed. In Section 8, the relationship between the coordinates used in the floating frame of reference formulation and the absolute nodal coordinate formulation is presented. This relationship is used in Section 9 to demonstrate the equivalence of the elastic forces used in the floating frame of reference formulation and the absolute nodal coordinate formulation. In Section 10, a Fourier analysis of the solution time history is used to shed more light on the fundamental problem of selecting the deformable body coordinate system in the floating frame of reference formulation [1, 4, 5, 9, 12, 16]. Summary and conclusions drawn from this study are presented in Section 11.

2 ABSOLUTE NODAL COORDINATE FORMULATION

The absolute nodal coordinate formulation is a non-incremental finite element procedure in which the coordinates of each node are defined in a fixed inertial coordinate system; hence no transformation matrices are required to define the kinematic position and velocity equations of the elements. Using the motion description of the absolute nodal coordinate formulation, a constant mass matrix is obtained for the finite elements. The element stiffness matrix, however, is a nonlinear function of the nodal coordinates. In this investigation the attention is focused on beam elements, which are not considered as isoparametric in the classical finite element formulations [10].

Referring to Fig. 2, the global position vector $\mathbf{r}$ of an arbitrary point P on the element is defined in terms of the nodal coordinates and the element shape function as

$$\mathbf{r} = \begin{bmatrix} r_1 \\ r_2 \end{bmatrix} = \mathbf{Se}, \tag{1}$$

where $\mathbf{S}$ is the global shape function which has a complete set of rigid body modes, and $\mathbf{e}$ is the vector of element nodal coordinates:

$$\mathbf{e} = \begin{bmatrix} e_1 & e_2 & e_3 & e_4 & e_5 & e_6 & e_7 & e_8 \end{bmatrix}^{\mathrm{T}}. \tag{2}$$

This vector of absolute nodal coordinates includes the global displacements

$$e_1 = r_1|_{x=0}, \quad e_2 = r_2|_{x=0}, \quad e_5 = r_1|_{x=l}, \quad e_6 = r_2|_{x=l}, \tag{3}$$

and the global slopes of the element nodes, that are defined as

$$e_3 = \left.\frac{\partial r_1}{\partial x}\right|_{x=0}, \quad e_4 = \left.\frac{\partial r_2}{\partial x}\right|_{x=0}, \quad e_7 = \left.\frac{\partial r_1}{\partial x}\right|_{x=l}, \quad e_8 = \left.\frac{\partial r_2}{\partial x}\right|_{x=l}. \tag{4}$$

Here x is the coordinate of an arbitrary point on the element in the undeformed configuration, and l is the original length of the beam.

Since absolute coordinates are used, a cubic polynomial is employed to describe both components of the displacements. Therefore, the global shape function $\mathbf{S}$ can be written as

$$\mathbf{S} = \begin{bmatrix} 1-3\xi^2+2\xi^3 & 0 & l(\xi-2\xi^2+\xi^3) & 0 & 3\xi^2-2\xi^3 & 0 & l(\xi^3-\xi^2) & 0 \\ 0 & 1-3\xi^2+2\xi^3 & 0 & l(\xi-2\xi^2+\xi^3) & 0 & 3\xi^2-2\xi^3 & 0 & l(\xi^3-\xi^2) \end{bmatrix}, \tag{5}$$

where $\xi = x/l$. It can be shown that this shape function contains a complete set of rigid body modes that can describe arbitrary rigid body translational and rotational displacements, provided that global slope coordinates are used instead of infinitesimal rotations. Using the absolute coordinates and slopes, it can also be shown that the beam element defined by the shape function of Eq. (5) is an isoparametric element.

Equations of motion Using the global position vector $\mathbf{r}$ defined in Eq. (1), the kinetic energy of the finite element can be defined as

$$T = \frac{1}{2}\int_V \rho \dot{\mathbf{r}}^{\mathrm{T}} \dot{\mathbf{r}} dV = \frac{1}{2}\dot{\mathbf{e}}^{\mathrm{T}} \left(\int_V \rho \mathbf{S}^{\mathrm{T}} \mathbf{S} dV \right) \dot{\mathbf{e}} = \frac{1}{2}\dot{\mathbf{e}}^{\mathrm{T}} \mathbf{M}_a \dot{\mathbf{e}}, \tag{6}$$

where ρ and V are the mass density and the volume of the element respectively, and $\mathbf{M}_a$ is the mass matrix defined as follows:

$$\mathbf{M}_a = \int_V \rho \mathbf{S}^{\mathrm{T}} \mathbf{S} dV. \tag{7}$$

This is a constant and symmetric matrix, obtained using a consistent mass approach. It can be shown [8] that this matrix leads to exact modeling of the rigid body inertia.

In order to develop the equations of motion of the element, the vector $\mathbf{Q}_k$ of the elastic forces and the vector $\mathbf{Q}_a$ of the externally applied forces must be defined. The vector $\mathbf{Q}_k$ can be defined using the strain energy U as follows:

$$\mathbf{Q}_k = \left(\frac{\partial U}{\partial \mathbf{e}} \right)^{\mathrm{T}}. \tag{8}$$

As it will be demonstrated later in this section, this vector is a highly nonlinear function of the vector of nodal coordinates $\mathbf{e}$, even when a simple linear elastic model is used.

The vector $\mathbf{Q}_a$, which contains the generalized external forces, including the gravity force, can be defined using the virtual work as

$$\delta W_e = \mathbf{Q}_a^{\mathrm{T}} \delta \mathbf{e}. \tag{9}$$

Using the expressions of the kinetic energy, strain energy, and the virtual work, the dynamic equations of the finite element can be obtained in a matrix form as follows:

$$\mathbf{M}_a \ddot{\mathbf{e}} + \mathbf{Q}_k = \mathbf{Q}_a, \tag{10}$$

where all the terms that appear in this equation have already been defined.

Elastic forces In order to demonstrate the nonlinearity of the elastic forces even when a simple linear elastic model is used, the classical Euler Bernoulli beam theory is used [20]. The strain energy due to the longitudinal and transverse deformations is given by

$$U = \frac{1}{2} \int_0^l \left[EA \left(\frac{\partial u_l}{\partial x} \right)^2 + EI \left(\frac{\partial^2 u_t}{\partial x^2} \right)^2 \right] dx, \tag{11}$$

where E is Young's modulus, A is the cross sectional area, I is the second moment of area, and u_l and u_t are respectively the longitudinal and transverse deflections as shown in Fig. 3.

Let $\mathbf{i}$ and $\mathbf{j}$ be unit vectors along the axes of the beam coordinate system. The following relationship holds for two-dimensional problems:

$$\mathbf{j} = \tilde{\mathbf{I}} \mathbf{i}, \tag{12}$$

where

$$\tilde{\mathbf{I}} = \begin{bmatrix} 0 & -1 \\ 1 & 0 \end{bmatrix}. \tag{13}$$

As shown in Fig. 3, the location of an arbitrary point P on the beam with respect to the origin O of the local frame x_1x_2 is defined by

$$\mathbf{u} = \mathbf{r}_P - \mathbf{r}_O = (\mathbf{S} - \mathbf{S}_O)\mathbf{e}, \tag{14}$$

where $\mathbf{S}$ is the shape matrix given by Eq. (5), and $\mathbf{S}_O$ is the shape matrix evaluated at the reference point O. The longitudinal and transverse deflections of point P can be defined as

$$\mathbf{u}_d = \begin{bmatrix} u_l \\ u_t \end{bmatrix} = \begin{bmatrix} \mathbf{u}^{\mathrm{T}}\mathbf{i} - x \\ \mathbf{u}^{\mathrm{T}}\mathbf{j} \end{bmatrix} = \begin{bmatrix} \mathbf{u}^{\mathrm{T}}\mathbf{i} - x \\ \mathbf{u}^{\mathrm{T}}\tilde{\mathbf{I}}\mathbf{i} \end{bmatrix}. \tag{15}$$

According to these definitions of the longitudinal and transverse deflections, the derivatives that appear in the strain energy expression of Eq. (11) are defined as follows:

$$\left(\frac{\partial u_l}{\partial x}\right) = \left(\frac{\partial \mathbf{u}}{\partial x}\right)^{\mathrm{T}} \mathbf{i} - 1 = (\mathbf{S}'\mathbf{e})^{\mathrm{T}}\mathbf{i} - 1 = \mathbf{e}^{\mathrm{T}}\mathbf{S}'^{\mathrm{T}}\mathbf{i} - 1, \tag{16}$$

and

$$\left(\frac{\partial^2 u_t}{\partial x^2}\right) = \left(\frac{\partial^2 \mathbf{u}}{\partial x^2}\right)^{\mathrm{T}} \tilde{\mathbf{I}}\mathbf{i} = (\mathbf{S}''\mathbf{e})^{\mathrm{T}}\tilde{\mathbf{I}}\mathbf{i}, \tag{17}$$

where

$$\mathbf{S}' = \frac{\partial \mathbf{S}}{\partial x}, \qquad \mathbf{S}'' = \frac{\partial^2 \mathbf{S}}{\partial x^2}. \tag{18}$$

By defining the following matrices

$$\mathbf{C}_1 = \int_0^l \mathbf{S}'^{\mathrm{T}}\mathbf{i}\,dx, \quad \mathbf{C}_2 = \int_0^l \mathbf{S}'^{\mathrm{T}}\mathbf{i}\cdot\mathbf{i}^{\mathrm{T}}\mathbf{S}'dx, \quad \mathbf{C}_3 = \int_0^l \mathbf{S}''^{\mathrm{T}}\tilde{\mathbf{I}}\mathbf{i}\cdot\mathbf{i}^{\mathrm{T}}\tilde{\mathbf{I}}^{\mathrm{T}}\mathbf{S}''dx, \tag{19}$$

the strain energy can be written as

$$U = \frac{1}{2}\left[EA(l - 2\mathbf{e}^{\mathrm{T}}\mathbf{C}_1 + \mathbf{e}^{\mathrm{T}}\mathbf{C}_2\mathbf{e}) + EI\mathbf{e}^{\mathrm{T}}\mathbf{C}_3\mathbf{e}\right]. \tag{20}$$

Clearly, this expression is not a quadratic form in the nodal coordinates vector $\mathbf{e}$, as in the case of linear structural mechanics. Equation (20) is a highly nonlinear function of the vector $\mathbf{e}$ because the unit vector $\mathbf{i}$ is a function of the nodal coordinates; that is $\mathbf{i} = \mathbf{i}(\mathbf{e})$. The form

of the matrices given in Eq. (19) and evaluated using the shape function of Eq. (5) are presented in the Appendix.

It is clear from the analysis presented in this section that the mass matrix that results from the use of the absolute nodal coordinate formulation takes a simple form. It is a constant and symmetric matrix , and it has the same form of the mass matrix used in linear structural dynamics. The elastic forces, on the other hand, have a much more complex expression as compared to the vector of elastic forces used in linear structural dynamics. It is one of the objectives of this investigation to establish a simple procedure for evaluating the nonlinear elastic forces of the absolute nodal coordinate formulation from the simple expression of the elastic forces used in linear structural dynamics. To this end, we first demonstrate that different element coordinate systems used to formulate the strain energy in the absolute nodal coordinate formulation lead to the same elastic forces, despite the fact that the definition of the longitudinal and transverse deformations depend on the choice of the coordinate system. As a consequence, the choice of the element coordinate system becomes immaterial in the absolute nodal coordinate formulation as the element size decreases. Using this result, we demonstrate in later sections the equivalence of the elastic forces used in the absolute nodal coordinate formulation and the floating frame of reference formulation, and use this equivalence to establish a simple procedure for defining the nonlinear elastic forces of the absolute nodal coordinate formulation from the simple expression of the elastic forces used in linear structural dynamics.

3 THE PINNED FRAME

In order to describe the deformation of a beam element in the absolute nodal coordinate formulation, several coordinate systems can be introduced. It is important, however, to emphasize that the use of a coordinate system in such a formulation is only for the purpose

of measuring the longitudinal and transverse displacements of a point on the element in order to evaluate the elastic forces. Therefore, such a local reference frame does not play the same role as in the case of the floating frame of reference formulation. For instance, the kinetic energy and the mass matrix used in the absolute nodal coordinate formulation were formulated in the preceding section without the need for any local coordinate system. Furthermore, it is theoretically possible to develop an expression for the strain energy and the vector of elastic forces following a continuum mechanics approach without the need for introducing a local reference frame.

In the floating frame of reference formulation [18], on the other hand, the deformation of the bodies is often described using elastic modes, and the elastic coordinates can be considered as the amplitudes of the modes. In this case, where low frequency modes are often used, the choice of the boundary conditions must be consistent with the choice of the local coordinate system.

In this section, we consider the case of a *pinned frame*, which has one of its axes passes through two nodes of the beam element as shown in Fig. 1b. The longitudinal and transverse deformations of the element are defined in this frame, and they are used to define the elastic forces in the absolute nodal coordinate formulation. In the following section, another frame known as the *tangent frame* is employed. The tangent frame can be viewed as an element-fixed coordinate system which has one of its axes tangent to the beam at one of the nodes as shown in Fig. 1a. In Section 5, a comparison between the pinned and the tangent frames is presented, and it is shown that the choice of such frames does not play a fundamental role in the absolute nodal coordinate formulation as in the case of the floating frame of reference formulation.

The pinned frame can be introduced by first defining the unit vector $\mathbf{i}$ along a line connecting point O (the origin of the coordinate system), and point A. Hence the unit

vector $\mathbf{i}$ is

$$\mathbf{i} = \begin{bmatrix} i_1 \\ i_2 \end{bmatrix} = \frac{\mathbf{r}_A - \mathbf{r}_O}{|\mathbf{r}_A - \mathbf{r}_O|}. \tag{21}$$

Using the definition of the vector $\mathbf{e}$ of Eqs. (2)-(4), one obtains

$$\mathbf{i} = \frac{1}{d} \begin{bmatrix} e_5 - e_1 \\ e_6 - e_2 \end{bmatrix}, \tag{22}$$

where d is the distance between the nodes at O and A defined as

$$d = \sqrt{(e_5 - e_1)^2 + (e_6 - e_2)^2}. \tag{23}$$

The derivatives $\boldsymbol{\psi}_1$ and $\boldsymbol{\psi}_2$ of i_1 and i_2 with respect to the nodal coordinates are

$$\boldsymbol{\psi}_1 = \left(\frac{\partial i_1}{\partial \mathbf{e}}\right)^{\mathrm{T}} = \frac{(i_2)^2}{d}\mathbf{I}_1 - \frac{i_1 i_2}{d}\mathbf{I}_2, \tag{24}$$

$$\boldsymbol{\psi}_2 = \left(\frac{\partial i_2}{\partial \mathbf{e}}\right)^{\mathrm{T}} = \frac{(i_1)^2}{d}\mathbf{I}_2 - \frac{i_1 i_2}{d}\mathbf{I}_1, \tag{25}$$

where the following vectors have been introduced

$$\mathbf{I}_1 = \begin{bmatrix} -1 & 0 & 0 & 0 & 1 & 0 & 0 & 0 \end{bmatrix}^{\mathrm{T}}, \quad \mathbf{I}_2 = \begin{bmatrix} 0 & -1 & 0 & 0 & 0 & 1 & 0 & 0 \end{bmatrix}^{\mathrm{T}}. \tag{26}$$

Substituting Eqs. (24)-(26) into Eq. (8), the vector of elastic forces can be written as

$$\begin{aligned} \mathbf{Q}_k = {} & \mathbf{D}\mathbf{e} - EA(i_1\mathbf{I}_1 + i_2\mathbf{I}_2) - EA(\mathbf{e}^{\mathrm{T}}\mathbf{I}_1)\boldsymbol{\psi}_1 - EA(\mathbf{e}^{\mathrm{T}}\mathbf{I}_2)\boldsymbol{\psi}_2 \\ & +(\mathbf{e}^{\mathrm{T}}\mathbf{D}_1\mathbf{e})i_1\boldsymbol{\psi}_1 + \frac{1}{2}(\mathbf{e}^{\mathrm{T}}\mathbf{D}_2\mathbf{e})(i_1\boldsymbol{\psi}_2 + i_2\boldsymbol{\psi}_1) + (\mathbf{e}^{\mathrm{T}}\mathbf{D}_3\mathbf{e})i_2\boldsymbol{\psi}_2, \end{aligned} \tag{27}$$

where the matrices $\mathbf{D}_1$, $\mathbf{D}_2$, $\mathbf{D}_3$ and $\mathbf{D}$ are defined as

$$\mathbf{D}_1 = EA\mathbf{C}_{21} + EI\mathbf{C}_{31}, \quad \mathbf{D}_2 = EA\mathbf{C}_{22} + EI\mathbf{C}_{32}, \quad \mathbf{D}_3 = EA\mathbf{C}_{23} + EI\mathbf{C}_{33}, \tag{28}$$

and

$$\mathbf{D} = (i_1)^2\mathbf{D}_1 + i_1 i_2\mathbf{D}_2 + (i_2)^2\mathbf{D}_3. \tag{29}$$

The matrices $\mathbf{C}_{ij}$ are defined in the Appendix.

4 THE TANGENT FRAME

In this section, a tangent frame that can be viewed as an element-fixed coordinate system is employed. This frame, shown in Fig. 3, has an origin rigidly attached to the node point O. In this case, the unit vector $\mathbf{i}$ that defines the x_1 axis of this frame is given by

$$\mathbf{i} = \frac{1}{\sqrt{(e_3)^2 + (e_4)^2}} \begin{bmatrix} e_3 \\ e_4 \end{bmatrix}. \tag{30}$$

Differentiation of the direction cosines i_1 and i_2 with respect to the vector of nodal coordinates gives

$$\boldsymbol{\varphi}_1 = \left(\frac{\partial i_1}{\partial \mathbf{e}}\right)^{\mathrm{T}} = \frac{(e_4)^2}{f^3}\mathbf{I}_3 - \frac{e_3 e_4}{f^3}\mathbf{I}_4, \tag{31}$$

$$\boldsymbol{\varphi}_2 = \left(\frac{\partial i_2}{\partial \mathbf{e}}\right)^{\mathrm{T}} = \frac{(e_3)^2}{f^3}\mathbf{I}_4 - \frac{e_3 e_4}{f^3}\mathbf{I}_3, \tag{32}$$

where

$$\mathbf{I}_3 = \begin{bmatrix} 0 & 0 & 1 & 0 & 0 & 0 & 0 & 0 \end{bmatrix}^{\mathrm{T}}, \quad \mathbf{I}_4 = \begin{bmatrix} 0 & 0 & 0 & 1 & 0 & 0 & 0 & 0 \end{bmatrix}^{\mathrm{T}}, \tag{33}$$

and

$$f = \sqrt{(e_3)^2 + (e_4)^2} = \left.\sqrt{\mathbf{r}'^{\mathrm{T}}\mathbf{r}'}\right|_{x=0}. \tag{34}$$

The quantity $\sqrt{\mathbf{r}'^{\mathrm{T}}\mathbf{r}'}$ plays the role of the longitudinal deformation gradient, so that the longitudinal strain is $\varepsilon_l = \frac{1}{2}(\mathbf{r}'^{\mathrm{T}}\mathbf{r}' - 1)$. Hence f gives a measure of the longitudinal deformation that occurs at the left end of the beam, at point O, and $f = 1$ in the case of no deformation. A similar comment applies to the other end of the beam element, therefore the information provided by the slopes is not only limited to information on the direction cosines.

The vector of elastic forces in the case of the tangent frame is

$$\begin{aligned} \mathbf{Q}_k = {} & \mathbf{De} - EA(i_1\mathbf{I}_1 + i_2\mathbf{I}_2) - EA(\mathbf{e}^{\mathrm{T}}\mathbf{I}_1)\boldsymbol{\varphi}_1 - EA(\mathbf{e}^{\mathrm{T}}\mathbf{I}_2)\boldsymbol{\varphi}_2 \\ & + (\mathbf{e}^{\mathrm{T}}\mathbf{D}_1\mathbf{e})i_1\boldsymbol{\varphi}_1 + \frac{1}{2}(\mathbf{e}^{\mathrm{T}}\mathbf{D}_2\mathbf{e})(i_1\boldsymbol{\varphi}_2 + i_2\boldsymbol{\varphi}_1) + (\mathbf{e}^{\mathrm{T}}\mathbf{D}_3\mathbf{e})i_2\boldsymbol{\varphi}_2, \end{aligned} \tag{35}$$

where the matrices that appear in this equation have already been defined by Eqs. (26), (28), (29), (31) and (32). Note that this expression of the elastic forces becomes identical to Eq. (27) if ψ_1 and ψ_2 are replaced by φ_1 and φ_2, respectively.

5 COMPARISON BETWEEN THE PINNED FRAME AND THE TANGENT FRAME

Numerical results are presented in this section in order to compare between the solutions obtained using the pinned and tangent frames. The study model used is the four-bar mechanism shown in Fig. 4. The mechanism consists of a crankshaft, a connecting rod (coupler), and a follower. The mechanism is driven by a moment applied to the crankshaft. The driving moment as a function of time is presented in Fig. 5. The inertia, geometric, and elastic properties of the components of the four-bar mechanism are shown in Table 1. The table shows the mass m, the cross sectional area A, the second moment of area I, the length l, and the modulus of elasticity E of the mechanism components.

The absolute nodal coordinate formulation is used to obtain the numerical results in the two cases of the pinned and tangent frames. Different finite element models that employ different numbers of elements are used in this numerical study. Note that a low value for the modulus of elasticity of the connecting rod is used in order to allow for the large deformation, which can be systematically simulated using the absolute nodal coordinate formulation. The results of the computer simulation are shown in Figs. 6-10. In all the four models used, one element is used for the crankshaft and four elements are used for the follower. In the first model, 6 elements are used for the coupler; in the second model, twelve elements are used for the coupler; in the third model, eighteen elements are used for the coupler, and in the fourth model thirty-six elements are used for the coupler. Therefore, the first model has 11 elements, the second model has 17 elements, the third model has 23 elements, and the

fourth model has 41 elements. The isoparametric beam elements used in this investigation are defined by the shape function of Eq. (5) and the vector of nodal coordinates of Eq. (2). All components of the four-bar mechanism are assumed to be made of uniform beams which are initially straight. The gravity effect is taken into consideration. Pin joints are used to describe the connectivity conditions between the components of the four-bar mechanism. In the absolute nodal coordinate formulation, the pin joint constraints take a very simple form as reported by Escalona et al [8].

The numerical results show that in general the pinned frame, as compared to the tangent frame, requires a less number of elements in order to achieve convergence. For instance, when the pinned frame is used, Model 3 in which the coupler is divided into 18 elements gives results which are in a good agreement with the results obtained by discretizing the coupler into 36 finite elements.

Figure 6 shows the results obtained using Model 1, which employs the least number of elements for the coupler. These results show that there is a significant difference between the solutions obtained using the pinned frame and the tangent frame when the large deformations of the coupler are considered.

Figures 7-9 show the effect of increasing the number of elements. It is clear from the results presented in these three figures that as the size of the elements decreases, better agreement between the two solutions is obtained. In particular, the results shown in Fig. 9 demonstrate that there are no significant differences between the two solutions when Model 4 is used.

Figure 10 shows the transverse deflection of the midpoint of the coupler using different models and different frames. The transverse deflection is determined as the distance of the midpoint to the straight line that connects the ends of the coupler. It is interesting to note that the model which has 17 elements (12 elements for the coupler) yields good results when the pinned frame is used. This is not the case when the tangent frame is considered. More

elements are required in order to achieve convergence. The good convergence characteristics of the pinned frame can be attributed to the fact that the deformation within the element as defined with respect to the element coordinate system remains small, despite the fact that the connecting rod undergoes large deformation. This is not the case when the tangent frame is used. The element deformations defined with respect to a coordinate system fixed to the end of the element are no longer small, as shown by Fig. 11. A computer animation of the motion of the four-bar mechanism is presented in Fig. 12. This computer animation is obtained using Model 4 and the pinned frame.

6 FLOATING FRAME OF REFERENCE FORMULATION

A conceptually different formulation from the absolute nodal coordinate formulation discussed in the preceding sections is the floating frame of reference formulation, which is widely used in flexible multibody dynamics. In the floating frame of reference formulation, a mixed set of absolute and local deformation coordinates are used to define the configuration of the deformable body. Each body in the multibody system is assigned a body coordinate system. The location and orientation of the body coordinate system in an inertial frame of reference are defined using a set of reference absolute Cartesian and orientation coordinates. The deformation of the body with respect to its coordinate system can be described using the finite element method. Since the element shape functions include rigid body modes, and since the finite displacements of the body are described using the reference coordinates, the rigid body modes of the shape function must be eliminated in order to define a unique displacement field. To this end, a set of reference conditions [18] which are consistent with the kinematic constraints imposed on the boundary of the deformable body are used. Therefore, in the floating frame of reference formulation the choice of the deformable body coordinate system plays a fundamental role in the formulation of the kinematic position, velocity and

acceleration equations. Furthermore, the degree of complexity of the inertia forces in the floating frame of reference formulation depends on the choice of the deformable body coordinate system [18]. This is not the case when the absolute nodal coordinate formulation is used.

In general, the floating frame of reference formulation leads to a simple expression for the elastic forces and a highly nonlinear expression for the inertia forces. The nonlinearity of the inertia forces is due to the coordinate transformation required to define the location of an arbitrary point on the body in the global inertial frame of reference. Such a coordinate transformation is not required in the absolute nodal coordinate formulation, and as a consequence, the mass matrix in the absolute nodal coordinate formulation takes a very simple form. Shabana and Schwertassek [17] demonstrated the equivalence of the inertia forces used in the absolute nodal coordinate formulation and the floating frame of reference formulation. It was shown that the nonlinear mass matrix of the floating frame of reference formulation can be systematically obtained from the constant mass matrix of the absolute nodal coordinate formulation. Crucial to proving this equivalence is the definition of the coordinates in the floating frame of reference formulation; local slopes instead of infinitesimal rotations must be used.

The fact that the stiffness matrix in the floating frame of reference formulation takes a simple form leads to the natural and interesting question of whether or not one can use this simple stiffness matrix to formulate the nonlinear elastic forces that appear in the absolute nodal coordinate formulation. In order to answer this question, one needs first to develop the relationship between the coordinates used in the absolute nodal coordinate formulation and the floating frame of reference formulation. Crucial to the success in developing this relationship is avoiding the kinematic linearization resulting from the use of the infinitesimal rotations as local deformation coordinates in the floating frame of reference formulation. Therefore, in the following section, local slopes instead of infinitesimal rotations are used

as deformation coordinates to formulate the strain energy in the floating frame of reference formulation. As it will be seen, the use of the slopes will slightly change the form of the strain energy.

7 STRAIN ENERGY IN THE FLOATING FRAME OF REFERENCE FORMULATION

In this section, an expression of the strain energy will be derived for beam elements using the floating frame of reference formulation in terms of local location coordinates instead of the familiar expression often obtained in terms of deformation coordinates. This new expression will be used in the following sections to formulate the nonlinear elastic forces in the absolute nodal coordinate formulation from the simple expression of the elastic forces used in the floating frame of reference formulation. To this end, a coordinate system that satisfies the simply supported end conditions is considered. The location and orientation of this coordinate system is identified using three coordinates; the position vector $\mathbf{R}$ of the origin O and the angle θ which defines the orientation of the beam coordinate system with respect to a global inertial system, as shown in Fig. 13. These three coordinates are the reference coordinates which can be written as

$$\mathbf{q}_r = \begin{bmatrix} \mathbf{R} \\ \theta \end{bmatrix}.$$

It follows that an arbitrary point P, whose position in the element coordinate system is given by the vector $\bar{\mathbf{u}}$, has the global position vector

$$\mathbf{r} = \mathbf{R} + \mathbf{A}\bar{\mathbf{u}}, \tag{36}$$

where $\mathbf{A}$ is the transformation matrix

$$\mathbf{A} = \begin{bmatrix} \cos\theta & -\sin\theta \\ \sin\theta & \cos\theta \end{bmatrix}. \tag{37}$$

In the case of a rigid body, the value of $\overline{\mathbf{u}}$ remains constant during the motion, while in the case of deformable bodies, $\overline{\mathbf{u}}$ depends on time and can be expressed in terms of a local shape-function matrix $\mathbf{S}_l$ and the vector of local coordinates $\mathbf{q}_l$ as follows:

$$\overline{\mathbf{u}} = \begin{bmatrix} \overline{u}_1 \\ \overline{u}_2 \end{bmatrix} = \mathbf{S}_l \mathbf{q}_l. \tag{38}$$

In order to be consistent with the assumed displacement field used previously in this paper for the absolute nodal coordinate formulation, the following local coordinates are employed for the beam element in the case of the floating frame of reference formulation:

$$\mathbf{q}_l = \begin{bmatrix} q_1 & q_2 & q_3 & q_4 & q_5 \end{bmatrix}^{\mathrm{T}}, \tag{39}$$

where

$$q_1 = \left.\frac{\partial \overline{u}_1}{\partial x}\right|_{x=0}, \quad q_2 = \left.\frac{\partial \overline{u}_2}{\partial x}\right|_{x=0}, \quad q_3 = \overline{u}_1(A), \quad q_4 = \left.\frac{\partial \overline{u}_1}{\partial x}\right|_{x=l}, \quad q_5 = \left.\frac{\partial \overline{u}_2}{\partial x}\right|_{x=l}, \tag{40}$$

in which point A is the right node of the beam element as shown in Fig. 13. Note that local slopes instead of infinitesimal rotations are employed, in order to avoid the linearization of the kinematic equations. The local shape function $\mathbf{S}_l$ is given by (with $\xi = x/l$):

$$\mathbf{S}_l = \begin{bmatrix} l(\xi - 2\xi^2 + \xi^3) & 0 & 3\xi^2 - 2\xi^3 & l(\xi^3 - \xi^2) & 0 \\ 0 & l(\xi - 2\xi^2 + \xi^3) & 0 & 0 & l(\xi^3 - \xi^2) \end{bmatrix}. \tag{41}$$

The deflections of an arbitrary point P in the case of the floating frame of reference formulation are given by

$$\mathbf{u}_d = \begin{bmatrix} u_l \\ u_t \end{bmatrix} = \begin{bmatrix} \overline{u}_1 - x \\ \overline{u}_2 \end{bmatrix}.$$

Using this equation, the expression of the strain energy U_f (where the subscript f refers to the floating frame of reference formulation) is identical to Eq. (11), which is repeated here for convenience:

$$U_f = \frac{1}{2}\int_0^l \left[EA\left(\frac{\partial u_l}{\partial x}\right)^2 + EI\left(\frac{\partial^2 u_t}{\partial x^2}\right)^2 \right] dx. \tag{42}$$

In this case,

$$\left(\frac{\partial u_l}{\partial x}\right) = \frac{\partial}{\partial x}(\mathbf{S}_{1l}\mathbf{q}_l - x) = \mathbf{S}'_{1l}\mathbf{q}_l - 1, \tag{43}$$

$$\left(\frac{\partial^2 u_t}{\partial x^2}\right) = \frac{\partial^2}{\partial x^2}\mathbf{S}_{2l}\mathbf{q}_l = \mathbf{S}''_{2l}\mathbf{q}_l, \tag{44}$$

where $\mathbf{S}_{1l}$ and $\mathbf{S}_{2l}$ are the first and the second rows of the local shape function matrix defined in Eq. (41), and the prime indicates derivation with respect to x. Substituting the preceding two equations into Eq. (42) leads to

$$U_f = \frac{1}{2}\int_0^l \left[EA\left(1 - 2\mathbf{S}'_{1l}\mathbf{q}_l + \mathbf{q}_l^{\mathrm{T}}\mathbf{S}'^{\mathrm{T}}_{1l}\mathbf{S}'_{1l}\mathbf{q}_l\right) + EI\mathbf{q}_l^{\mathrm{T}}\mathbf{S}''^{\mathrm{T}}_{2l}\mathbf{S}''_{2l}\mathbf{q}_l\right] dx. \tag{45}$$

Let

$$\mathbf{K}_0 = EAl\int_0^1 \mathbf{S}'^{\mathrm{T}}_{1l} d\xi = EA\begin{bmatrix} 0 & 0 & 1 & 0 & 0 \end{bmatrix}^{\mathrm{T}}, \tag{46}$$

$$\mathbf{K}_1 = EAl\int_0^1 \mathbf{S}'^{\mathrm{T}}_{1l}\mathbf{S}'_{1l} d\xi = \frac{EA}{l}\begin{bmatrix} 2l^2/15 & 0 & -l/10 & -l^2/30 & 0 \\ 0 & 0 & 0 & 0 & 0 \\ -l/10 & 0 & 6/5 & -l/10 & 0 \\ -l^2/30 & 0 & -l/10 & 2l^2/15 & 0 \\ 0 & 0 & 0 & 0 & 0 \end{bmatrix}, \tag{47}$$

$$\mathbf{K}_2 = EIl\int_0^1 \mathbf{S}''^{\mathrm{T}}_{2l}\mathbf{S}''_{2l} d\xi = \frac{EI}{l^3}\begin{bmatrix} 0 & 0 & 0 & 0 & 0 \\ 0 & 4l^2 & 0 & 0 & 2l^2 \\ 0 & 0 & 0 & 0 & 0 \\ 0 & 0 & 0 & 0 & 0 \\ 0 & 2l^2 & 0 & 0 & 4l^2 \end{bmatrix}. \tag{48}$$

Using these definitions, the expression of the strain energy can be simply written as

$$U_f = \frac{1}{2}EAl - \mathbf{K}_0^{\mathrm{T}}\mathbf{q}_l + \frac{1}{2}\mathbf{q}_l^{\mathrm{T}}(\mathbf{K}_1 + \mathbf{K}_2)\mathbf{q}_l. \tag{49}$$

Note that the strain energy contains the linear term $\frac{1}{2}EAl - \mathbf{K}_0^{\mathrm{T}}\mathbf{q}_l$. Therefore, the strain energy is not a simple quadratic form of the local coordinates. This is mainly due to the fact

that the local coordinates, as defined in Eq. (38), describe the local position of an arbitrary point P in the undeformed state as well as the deformation of this point. When coordinates that only account for deformations are used, the simple and familiar quadratic form of the strain energy can be obtained.

8 RELATIONSHIP BETWEEN THE COORDINATES

In this section, a relationship between the coordinates used in the absolute nodal coordinate formulation and the floating frame of reference formulation is presented. This relationship will be used in the following section to obtain the nonlinear elastic forces in the absolute nodal coordinate formulation from the simple expression of the elastic forces in the floating frame of reference approach.

Using Eq. (40), it can be shown that the nodal coordinates of the absolute nodal coordinate formulation can be expressed in terms of the coordinates used in the floating frame of reference formulation as

$$\mathbf{e} = \begin{bmatrix} e_1 \\ e_2 \\ e_3 \\ e_4 \\ e_5 \\ e_6 \\ e_7 \\ e_8 \end{bmatrix} = \begin{bmatrix} R_1 \\ R_2 \\ q_1 \cos\theta - q_2 \sin\theta \\ q_1 \sin\theta + q_2 \cos\theta \\ R_1 + q_3 \cos\theta \\ R_2 + q_3 \sin\theta \\ q_4 \cos\theta - q_5 \sin\theta \\ q_4 \sin\theta + q_5 \cos\theta \end{bmatrix} = \mathbf{e}(\mathbf{q}_r, \mathbf{q}_l). \tag{50}$$

Using Fig. 14, it can be shown that the inverse relationship is

$$\left.\begin{aligned} q_1 &= e_3 \cos\theta + e_4 \sin\theta \\ q_2 &= -e_3 \sin\theta + e_4 \cos\theta \\ q_3 &= (e_5 - e_1)\cos\theta + (e_6 - e_2)\sin\theta \\ q_4 &= e_7 \cos\theta + e_8 \sin\theta \\ q_5 &= -e_7 \sin\theta + e_8 \cos\theta \end{aligned}\right\}, \tag{51}$$

where the angle θ can be expressed as a function of the vector $\mathbf{e}$ using Eq. (22). Equation (51) can be written in a matrix form as

$$\mathbf{q}_l = \mathbf{Be}, \tag{52}$$

where

$$\mathbf{B} = \begin{bmatrix} 0 & 0 & \cos\theta & \sin\theta & 0 & 0 & 0 & 0 \\ 0 & 0 & -\sin\theta & \cos\theta & 0 & 0 & 0 & 0 \\ -\cos\theta & -\sin\theta & 0 & 0 & \cos\theta & \sin\theta & 0 & 0 \\ 0 & 0 & 0 & 0 & 0 & 0 & \cos\theta & \sin\theta \\ 0 & 0 & 0 & 0 & 0 & 0 & -\sin\theta & \cos\theta \end{bmatrix}. \tag{53}$$

9 ELASTIC FORCES

It is shown in this section, using the coordinate relationship presented in the preceding section, that the nonlinear elastic forces used in the absolute nodal coordinate formulation can be systematically obtained using the simple expression of the elastic forces used in the floating frame of reference formulation. To this end, Eq. (52) is substituted into Eq. (49) leading to

$$U_f = \frac{1}{2}EAl - \mathbf{K}_0^{\mathrm{T}}\mathbf{Be} + \frac{1}{2}\mathbf{e}^{\mathrm{T}}\mathbf{B}^{\mathrm{T}}(\mathbf{K}_1 + \mathbf{K}_2)\mathbf{Be}. \tag{54}$$

Using the following definitions:

$$c = \cos\theta, \qquad s = \sin\theta, \tag{55}$$

$$\mathbf{K}_{l0} = \mathbf{B}^{\mathrm{T}}\mathbf{K}_0 = EA\begin{bmatrix} -c & -s & 0 & 0 & c & s & 0 & 0 \end{bmatrix}^{\mathrm{T}}, \tag{56}$$

$$\mathbf{K}_l = \mathbf{B}^{\mathrm{T}}\mathbf{K}_1\mathbf{B} = \frac{EA}{l}\frac{1}{30}\begin{bmatrix} 36c^2 & 36cs & 3lc^2 & 3lcs & -36c^2 & -36cs & 3lc^2 & 3lcs \\ & 36s^2 & 3lcs & 3ls^2 & -36cs & -36S^2 & 3lcs & 3ls^2 \\ & & 4l^2c^2 & 4l^2cs & -3lc^2 & -3lcs & -l^2c^2 & -l^2cs \\ & & & 4l^2s^2 & -3lcs & -3ls^2 & -l^2cs & -l^2s^2 \\ & & & & 36c^2 & 36cs & -3lc^2 & -3lcs \\ & & & & & 36s^2 & -3lcs & -3ls^2 \\ & & symm. & & & & 4l^2c^2 & 4l^2cs \\ & & & & & & & 4l^2s^2 \end{bmatrix}, \tag{57}$$

$$\mathbf{K}_t = \mathbf{B}^{\mathrm{T}}\mathbf{K}_2\mathbf{B} = \frac{EI}{l^3}\begin{bmatrix} 0 & 0 & 0 & 0 & 0 & 0 & 0 & 0 \\ & 0 & 0 & 0 & 0 & 0 & 0 & 0 \\ & & 4l^2s^2 & -4l^2cs & 0 & 0 & 2l^2s^2 & -2l^2cs \\ & & & 4l^2c^2 & 0 & 0 & -2l^2cs & 2l^2c^2 \\ & & & & 0 & 0 & 0 & 0 \\ & & & & & 0 & 0 & 0 \\ & & symm. & & & & 4l^2s^2 & -4l^2cs \\ & & & & & & & 4l^2c^2 \end{bmatrix}, \tag{58}$$

the strain energy can be written as

$$U_f = \frac{1}{2}\left[EAl - 2\mathbf{K}_{l0}^{\mathrm{T}}\mathbf{e} + \mathbf{e}^{\mathrm{T}}(\mathbf{K}_l + \mathbf{K}_t)\mathbf{e}\right]. \tag{59}$$

It can be shown that this expression for the strain energy is the same as the strain energy U of Eq. (20) obtained in the case of the absolute nodal coordinate formulation. Considering the expression of the matrices $\mathbf{C}_1$, $\mathbf{C}_2$, and $\mathbf{C}_3$ presented in the Appendix, it can be shown that $\mathbf{K}_{l0} = EA\mathbf{C}_1$ and $\mathbf{K}_l = EA\mathbf{C}_2$. However, $\mathbf{K}_t \neq EI\mathbf{C}_3$. On the other hand, the simple structure of matrix $\mathbf{K}_t$ is consistent with the type of reference frame used for the evaluation of the longitudinal and transverse deflections. The reference frame used satisfies the simply-supported end conditions, and as such, a variation in the coordinates of the end points, say

O and A, makes a variation in the rotation θ of the frame, but does not affect the transverse deflections which depend only on the slopes. This explains why $\mathbf{K}_t$ has zeros in all the positions not related to the slopes.

In order to prove that the expression of the strain energy given by Eq. (59) is the same as the one given by Eq. (20), it is enough to show that $\mathbf{e}^{\mathrm{T}}(\mathbf{K}_t - EI\mathbf{C}_3)\mathbf{e}$ is identically equal to zero for every $\mathbf{e}$ and for every length l. This can be easily demonstrated by carrying out the matrix multiplication, and noting that the coordinates of node A can be written as $e_5 = e_1 + d\cos\theta$ and $e_6 = e_2 + d\sin\theta$, d being the distance between the nodes as shown in Fig. 14.

Straightforward differentiation of U_f with respect to the nodal coordinates gives the expression of the elastic forces. Note that instead of calculating the derivatives of $\mathbf{K}_{l0}$, $\mathbf{K}_l$ and $\mathbf{K}_t$ with respect to θ, it is more convenient to differentiate with respect to c and s, where $c = \cos\theta$, $s = \sin\theta$. The result of this differentiation is

$$\begin{aligned}\left(\frac{\partial U_f}{\partial \mathbf{e}}\right)^{\mathrm{T}} &= -\mathbf{K}_{l0} - (\mathbf{e}^{\mathrm{T}}\mathbf{K}_{l0,c})\boldsymbol{\psi}_1 - (\mathbf{e}^{\mathrm{T}}\mathbf{K}_{l0,s})\boldsymbol{\psi}_2 \\ &\quad +\mathbf{K}_l\mathbf{e} + \frac{1}{2}(\mathbf{e}^{\mathrm{T}}\mathbf{K}_{l,c}\mathbf{e})\boldsymbol{\psi}_1 + \frac{1}{2}(\mathbf{e}^{\mathrm{T}}\mathbf{K}_{l,s}\mathbf{e})\boldsymbol{\psi}_2 \\ &\quad +\mathbf{K}_t\mathbf{e} + \frac{1}{2}(\mathbf{e}^{\mathrm{T}}\mathbf{K}_{t,c}\mathbf{e})\boldsymbol{\psi}_1 + \frac{1}{2}(\mathbf{e}^{\mathrm{T}}\mathbf{K}_{t,s}\mathbf{e})\boldsymbol{\psi}_2,\end{aligned} \tag{60}$$

where

$$(\ )_{,c} = \frac{\partial}{\partial c}, \quad (\ )_{,s} = \frac{\partial}{\partial s}, \quad \boldsymbol{\psi}_1 = \left(\frac{\partial c}{\partial \mathbf{e}}\right)^{\mathrm{T}}, \quad \boldsymbol{\psi}_2 = \left(\frac{\partial s}{\partial \mathbf{e}}\right)^{\mathrm{T}}.$$

Here $\boldsymbol{\psi}_1$ and $\boldsymbol{\psi}_2$ are the same vectors defined by Eqs. (24) and (25), since $c = i_1$ and $s = i_2$. Note that Eq. (60) yields the same results as Eq. (27), as a consequence of the equivalence of the expressions of the strain energy used in the two formulations.

It is also important to point out that starting with Eq. (50), a velocity transformation matrix can be defined and used to obtain a relation similar to Eq. (52), but with a matrix $\mathbf{B}$ depending on $\mathbf{q}_l$ as well as θ. This approach leads to a more complicated expression for the elastic forces. On the other hand, the approach used in this section leads to a matrix $\mathbf{B}$

that depends only on θ.

10 FREQUENCIES AND BOUNDARY CONDITIONS

The equivalence of the two finite element formulations discussed in the preceding sections can be used to shed more light on the fundamental problem of selecting the deformable body coordinate system in the floating frame of reference formulation. In the absolute nodal coordinate formulation, a full finite element representation is used. In this case, large deformation problems can be examined as previously demonstrated by the results of the four-bar example presented in this paper. The floating frame of reference formulation, on the other hand, has been primarily used for the small deformation analysis. This is due to the fact that non-isoparametric beam and plate elements, which employ infinitesimal rotations, have been often used with the floating frame of reference formulation. Mode reduction techniques have been also used with the floating frame of reference formulation in order to reduce the number of elastic degrees of freedom.

In the floating frame of reference formulation interesting and fundamental issues related to the choice of the boundary conditions, mode shapes and deformable body coordinate systems must be addressed [16]. Different sets of mode shapes that correspond to different sets of end conditions and natural frequencies can be chosen for a flexible link to yield approximately the same results as previously demonstrated [16].

For example, the deformation of the connecting rod of the four-bar mechanism shown in Fig. 4 can be modeled using mode shapes obtained from simply supported end conditions, free-free end conditions, or double cantilever end conditions. The first six mode shapes and the corresponding natural frequencies using these different end conditions of the connecting rod are shown in Table 2 [6]. The results presented in Table 2 are obtained using the dimensions and material properties of the connecting rod reported in Section 5, with the

exception of the moduli of elasticity. For the connecting rod, E is increased to 0.5E10 MPa in order to obtain small deformations and justify the use of the linear model; for the crankshaft, E is increased to 1.0E10 MPa; and for the follower, E is increased to 5.0E10 MPa.

As demonstrated in previous publications, the simulation results obtained using these end conditions agree well [16]. Figure 15 shows a comparison between the results obtained using the floating frame of reference formulation and the absolute nodal coordinate formulation for the midpoint deflection of the connecting rod. The results of the floating frame of reference formulation are obtained using the simply supported end conditions and six modes of vibrations. It is clear from this figure that there is a good agreement between the results obtained using the two formulations.

With this good agreement, it is possible to examine the frequency content in the solution obtained using the absolute nodal coordinate formulation which does not employ modes. These frequency contents can be compared with the natural frequencies presented in Table 2 in order to see if there is any correlation between the natural frequencies of the linear problem and the frequency contents in the solution of the nonlinear multibody problem. Figure 16 shows the Fourier transform of the solution for the midpoint deflection of the connecting rod. Several frequencies appear to be significant from the results presented in this figure. It is difficult, however, to draw any correlation between the frequency content in the solution and the natural frequencies obtained using the boundary conditions specified in Table 2. These results show that in the floating frame of reference formulation, it is important to choose the boundary conditions that yield a shape of deformation consistent with the kinematic constraints imposed on the motion of the deformable body. However, there is no relationship between the natural frequencies of the linear problem that result from imposing these boundary conditions and the frequency content in the solution of the nonlinear problem.

11 SUMMARY AND CONCLUSIONS

The floating frame of reference formulation is widely used in flexible multibody simulations. In this formulation, a coordinate system is assigned to each flexible body in the multibody system. The location and orientation of this body coordinate system are defined using absolute Cartesian and orientation coordinates. The deformations of the body with respect to its coordinate system are defined using local coordinates that can be introduced using the finite element method. It was observed, in high speed rotor craft applications, that the solutions obtained using the floating frame of reference formulation incorrectly exhibit instability problems when the angular velocity of the flexible body exceeds a certain limit. This incorrect solution was attributed to the neglect of the centrifugal geometric stiffening effect. Studies which include the geometric stiffening effect or employ a nonlinear elastic model showed that the instability problem can be solved. There has been an argument, however, that the instability problem is a characteristic of the floating frame of reference formulation and can be avoided using a full finite element representation which does not account for the geometric centrifugal stiffening effect nor the elastic nonlinearity.

The analysis presented in this paper demonstrates otherwise. To this end, the absolute nodal coordinate formulation which employs a full finite element representation is used. Unlike the floating frame of reference formulation, in the absolute nodal coordinate formulation global position and slope coordinates are used. The formulation leads to a constant mass matrix and a highly nonlinear vector of elastic forces. Using the absolute nodal coordinate formulation, it was demonstrated that the generalized elastic forces obtained using the full finite element representation are equivalent to the elastic forces obtained using the floating frame of reference formulation, thereby demonstrating that the instability problem resulting form the neglect of the geometric centrifugal stiffening effect is not a problem inherent to only the floating frame of reference formulation.

The results of the analysis presented in this paper with the results previously reported

[17] clearly demonstrate that all the forces used in the floating frame of reference formulation can be obtained from the forces resulting from the use of a full finite element representation by simply using coordinate transformation, provided that no linearization of the kinematic equations is employed. Using the equivalence between the absolute nodal coordinate formulation and the floating frame of reference formulation, the fundamental problem of selecting the deformable body coordinate system in the floating frame of reference formulation is discussed.

APPENDIX

The stiffness shape integrals that appear in Eq. (19) are as follows:

$$\mathbf{C}_1 = i_1\mathbf{I}_1 + i_2\mathbf{I}_2, \quad \mathbf{C}_2 = (i_1)^2\mathbf{C}_{21} + i_1 i_2\mathbf{C}_{22} + (i_2)^2\mathbf{C}_{23}, \quad \mathbf{C}_3 = (i_1)^2\mathbf{C}_{31} + i_1 i_2\mathbf{C}_{32} + (i_2)^2\mathbf{C}_{33},$$

where

$$\mathbf{C}_{21} = \frac{1}{l}\begin{bmatrix} \frac{6}{5} & 0 & \frac{l}{10} & 0 & -\frac{6}{5} & 0 & \frac{l}{10} & 0 \\ & 0 & 0 & 0 & 0 & 0 & 0 & 0 \\ & & \frac{2l^2}{15} & 0 & -\frac{l}{10} & 0 & -\frac{l^2}{30} & 0 \\ & & & 0 & 0 & 0 & 0 & 0 \\ & & & & \frac{6}{5} & 0 & -\frac{l}{10} & 0 \\ & & \mathit{sym.} & & & 0 & 0 & 0 \\ & & & & & & \frac{2l^2}{15} & 0 \\ & & & & & & & 0 \end{bmatrix},$$

$$\mathbf{C}_{22} = \frac{1}{l}\begin{bmatrix} 0 & \frac{6}{5} & 0 & \frac{l}{10} & 0 & -\frac{6}{5} & 0 & \frac{l}{10} \\ & 0 & \frac{l}{10} & 0 & -\frac{6}{5} & 0 & \frac{l}{10} & 0 \\ & & 0 & \frac{2l^2}{15} & 0 & -\frac{l}{10} & 0 & -\frac{l^2}{30} \\ & & & 0 & -\frac{l}{10} & 0 & -\frac{l^2}{30} & 0 \\ & & & & 0 & \frac{6}{5} & 0 & -\frac{l}{10} \\ & & \mathit{sym.} & & & 0 & -\frac{l}{10} & 0 \\ & & & & & & 0 & \frac{2l^2}{15} \\ & & & & & & & 0 \end{bmatrix},$$

$$
\mathbf{C}_{23} = \frac{1}{l}\begin{bmatrix}
0 & 0 & 0 & 0 & 0 & 0 & 0 & 0 \\
 & \frac{6}{5} & 0 & \frac{L}{10} & 0 & -\frac{6}{5} & 0 & \frac{l}{10} \\
 & & 0 & 0 & 0 & 0 & 0 & 0 \\
 & & & \frac{2l^2}{15} & 0 & -\frac{l}{10} & 0 & -\frac{l^2}{30} \\
 & & & & 0 & 0 & 0 & 0 \\
 & & sym. & & & \frac{6}{5} & 0 & -\frac{l}{10} \\
 & & & & & & 0 & 0 \\
 & & & & & & & \frac{2l^2}{15}
\end{bmatrix},
$$

$$
\mathbf{C}_{31} = \frac{1}{l^3}\begin{bmatrix}
0 & 0 & 0 & 0 & 0 & 0 & 0 & 0 \\
 & 12 & 0 & 6l & 0 & -12 & 0 & 6l \\
 & & 0 & 0 & 0 & 0 & 0 & 0 \\
 & & & 4l^2 & 0 & -6l & 0 & 2l^2 \\
 & & & & 0 & 0 & 0 & 0 \\
 & & sym. & & & 12 & 0 & -6l \\
 & & & & & & 0 & 0 \\
 & & & & & & & 4l^2
\end{bmatrix},
$$

$$
\mathbf{C}_{32} = \frac{1}{l^3}\begin{bmatrix}
0 & -12 & 0 & -6l & 0 & 12 & 0 & -6l \\
 & 0 & -6l & 0 & 12 & 0 & -6l & 0 \\
 & & 0 & -4l^2 & 0 & 6l & 0 & -2l^2 \\
 & & & 0 & 6l & 0 & -2l^2 & 0 \\
 & & & & 0 & -12 & 0 & 6l \\
 & & sym. & & & 0 & 6l & 0 \\
 & & & & & & 0 & -4l^2 \\
 & & & & & & & 0
\end{bmatrix},
$$

$$\mathbf{C}_{33} = \frac{1}{l^3} \begin{bmatrix} 12 & 0 & 6l & 0 & -12 & 0 & 6l & 0 \\ & 0 & 0 & 0 & 0 & 0 & 0 & 0 \\ & & 4l^2 & 0 & -6l & 0 & 2l^2 & 0 \\ & & & 0 & 0 & 0 & 0 & 0 \\ & & & & 12 & 0 & -6l & 0 \\ & & sym. & & & 0 & 0 & 0 \\ & & & & & & 4l^2 & 0 \\ & & & & & & & 0 \end{bmatrix} .$$

REFERENCES

[1] Ashley H., 'Observations on the Dynamic Behavior of Large Flexible Bodies in Orbit', *AIAA Journal* **5**(3), 1967, 460-469

[2] Avello A., De Jalon G. and Bayo E., 'Dynamics of flexible multibody systems using Cartesian co-ordinates and large displacement theory', *Int. Journal for Numerical Methods in Engineering* **32**(8), 1991, 1543-1564

[3] Belytschko T. and Hsieh B.J., 'Non-linear transient finite element analysis with convected co-ordinates', *Int. Journal for Numerical Methods in Engineering* **7**, 1973, 255-271

[4] Canavin J.R. and Likins P.W., 'Floating Reference Frames for Flexible Spacecrafts', *Journal of Spacecraft* **14**(12), 1977, 724-732

[5] De Veubeke B.F., 'The dynamics of flexible bodies', *Int. Journal for Engineering Science* **14**, 1976, 895-913

[6] Den Hartog J.P., *Mechanical Vibrations*, Dover Publications, 1985

[7] El-Absy H. and Shabana A.A., 'Geometric stiffness and stability of rigid body modes', *Journal of Sound and Vibration* **207**(4), 1997, 465-496

[8] Escalona J.L., Hussien H.A. and Shabana A.A., 'Application of the absolute nodal coordinate formulation to multibody system dynamics', *Journal of Sound and Vibration* **214**(5), 1998, 833-851

[9] Friberg O., 'A method for selecting deformation modes in flexible multibody dynamics', *Int. Journal for Numerical Methods in Engineering* **32**(8), 1991 1637-1656

[10] Hughes T.J.R., *The Finite Element Method*, Prentice-Hall, 1987

[11] Kane T.R., Ryan R.R. and Banerjee A.K., 'Dynamics of a cantilever beam attached to a moving base', *AIAA Journal of Guidance, Control, and Dynamics* **10**(2), 1987, 139-151

[12] Koppens W.P., 'The dynamics of systems of deformable bodies', Ph.D. Thesis, Technical University of Eindhoven, The Netherlands, 1989

[13] Likins P.W., 'Modal method for analysis of free rotations of spacecraft', *AIAA Journal* **5**(7), 1967, 1304-1308

[14] Mayo J., 'Geometrically nonlinear formulations of flexible multibody dynamics', Ph.D. Thesis, University of Seville, Spain 1993

[15] Rankin C.C. and Brogan F.A., 'An element independent corotational procedure for the treatment of large rotations', *ASME Journal of Pressure Vessel Technology* **108**, 1986, 165-174

[16] Shabana A.A., 'Resonance conditions and deformable body coordinate systems', *Journal of Sound and Vibration* **192**(1), 1996, 389-398

[17] Shabana A.A. and Schwertassek R., 'Equivalence of the floating frame of reference approach and finite element formulations', *Int. Journal of Non-Linear Mechanics* **33**(3), 1998, 417-432

[18] Shabana A.A., *Dynamics of Multibody Systems*, 2nd Ed., Cambridge University Press, 1998

[19] Simo J.C. and Vu-Quoc L., 'On the Dynamics of Flexible Beams Under Large Overall Motions-The Plane Case: Part I', *Journal of Applied Mechanics* **53**, Dec. 1986, 849-854

[20] Timoshenko S., *Theory of elasticity*, 3rd Ed., New York McGraw-Hill, 1987

Table 1. Parameters used in the simulation of the four-bar mechanism

Body	m [kg]	A [m^2]	I [m^4]	l [m]	E [MPa]
Crankshaft	0.6811	1.257E-03	1.257E-07	0.2	1.000E+09
Coupler	2.4740	1.960E-03	3.068E-07	0.9	5.000E+06
Follower	1.4700	7.068E-03	3.976E-08	0.5196174	5.000E+08

Table 2. Mode shapes and natural frequencies for different boundary conditions

	Simply supported		Double cantilever		Free-free(*)	
Mode	**Shape**	**Freq. [Hz]**	**Shape**	**Freq. [Hz]**	**Shape**	**Freq. [Hz]**
1		45.81		65.28		103.85
2		183.24		65.28		286.26
3		412.30		409.10		561.19
4	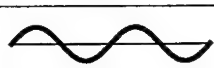	732.97		409.10		927.67
5	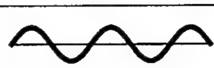	1145.27		1145.50	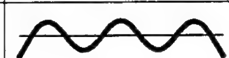	1385.78
6	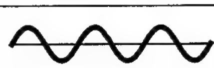	1649.19		1145.50		1935.51

(*) The rigid body mode is not reported in this table

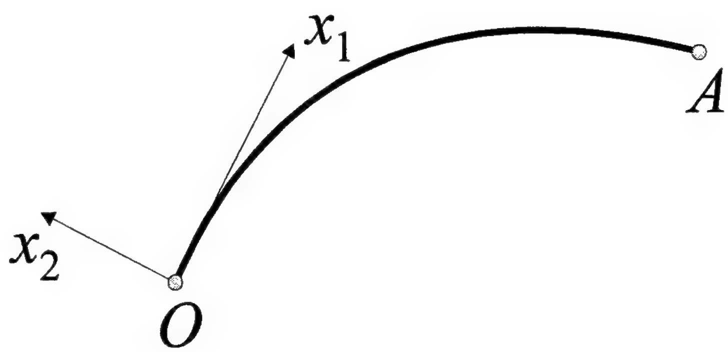

***a*)** Tangent coordinate system

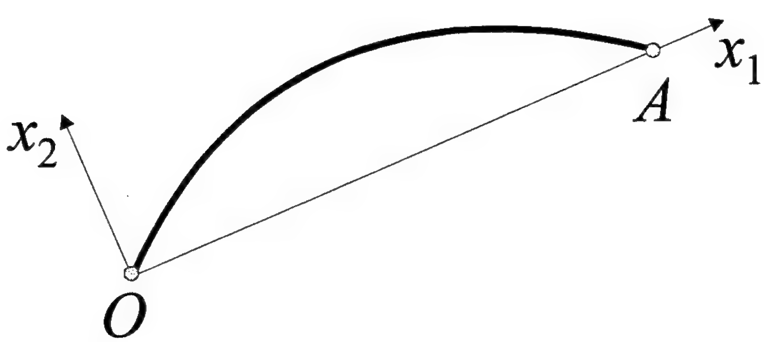

***b*)** Pinned coordinate system

Fig. 1. The tangent and the pinned coordinate systems

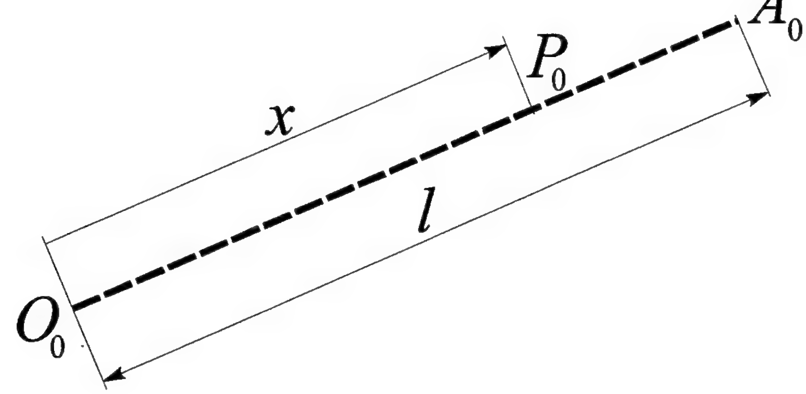

***a*)** Undeformed configuration

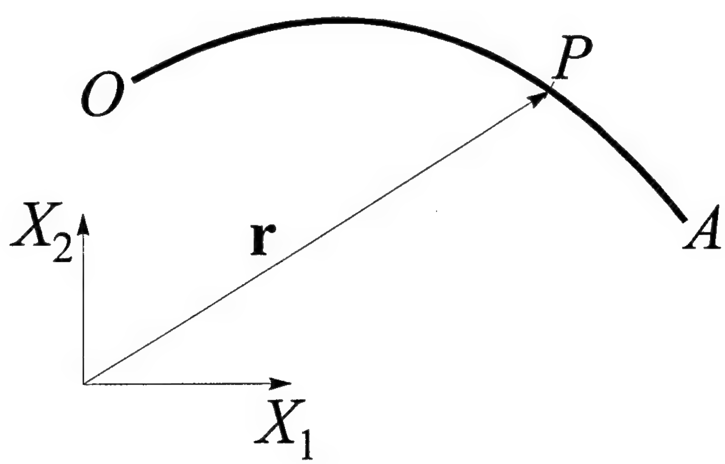

***b*)** Deformed configuration

Fig. 2. Undeformed and deformed configurations

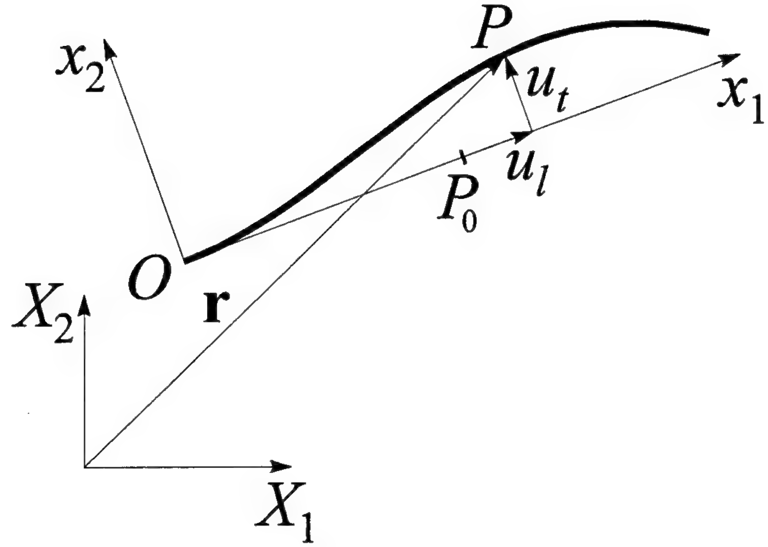

Fig. 3. Deformations defined in the tangent coordinate system

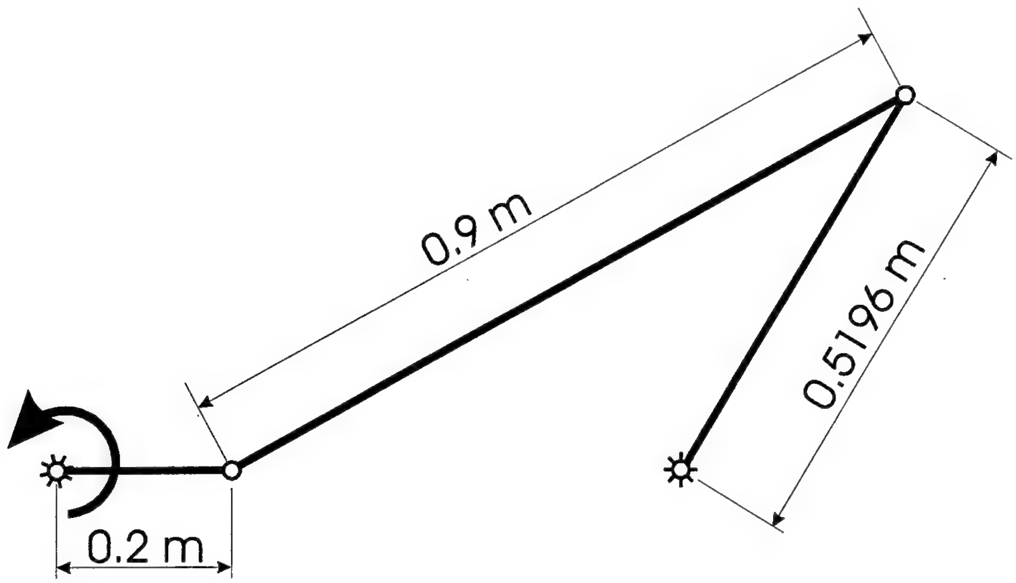

Fig. 4. Four-bar mechanism

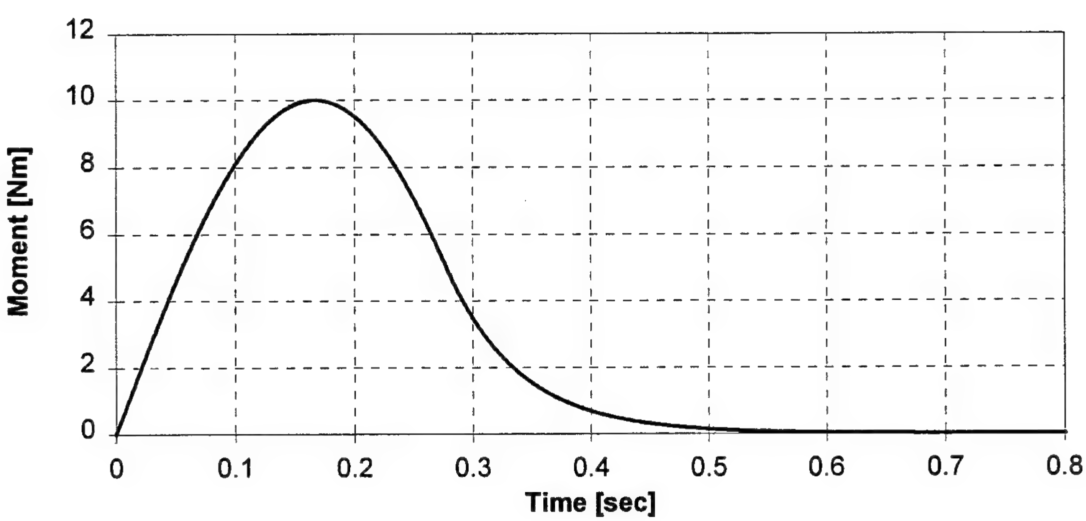

Fig. 5. Moment applied to the crankshaft

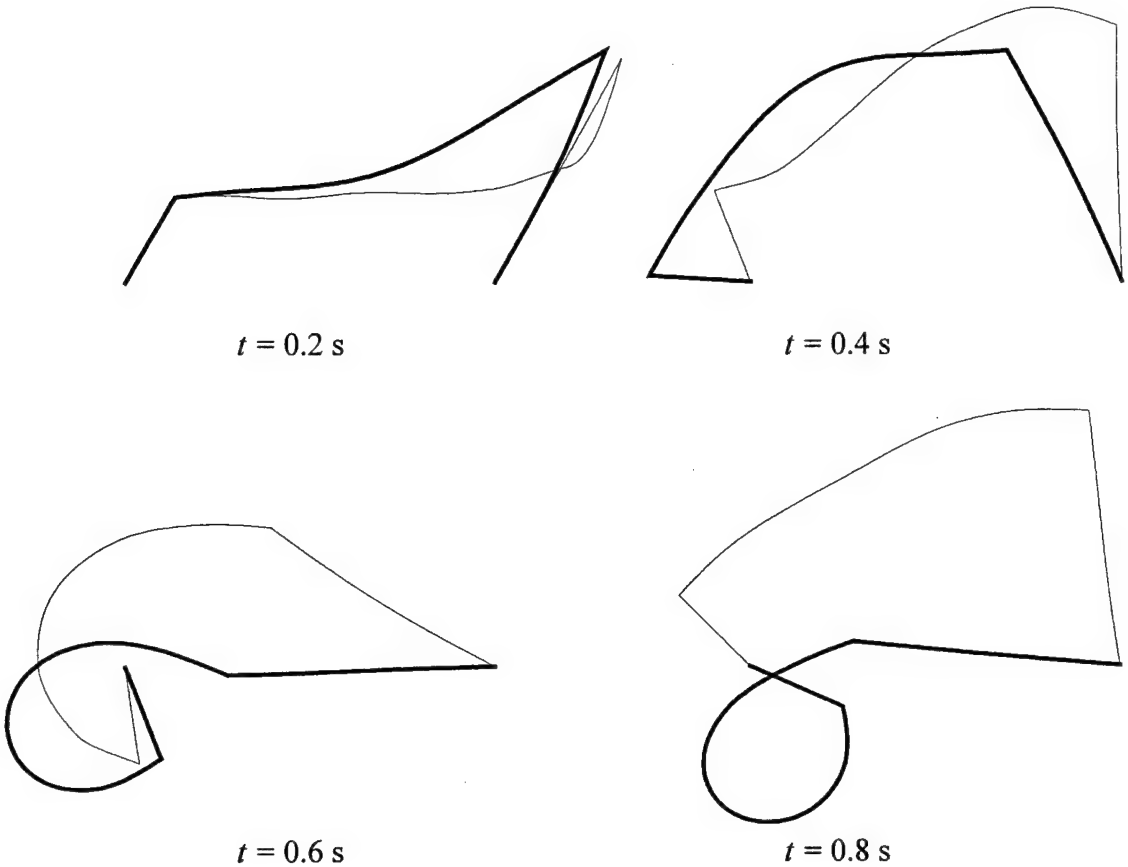

Fig. 6. Large deformations of the four-bar mechanism
— Model 1 with pinned frame
— Model 1 with tangent frame

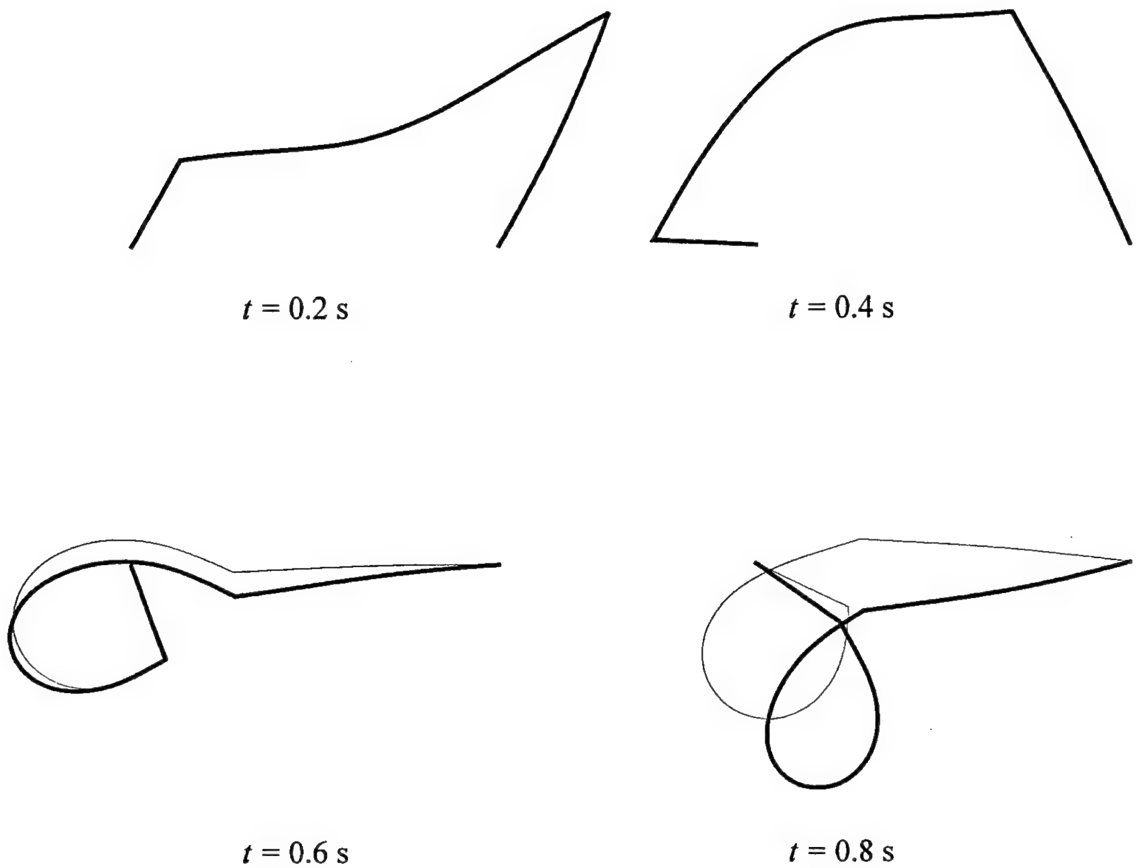

Fig. 7. Large deformations of the four-bar mechanism
— Model 2 with pinned frame
— Model 2 with tangent frame

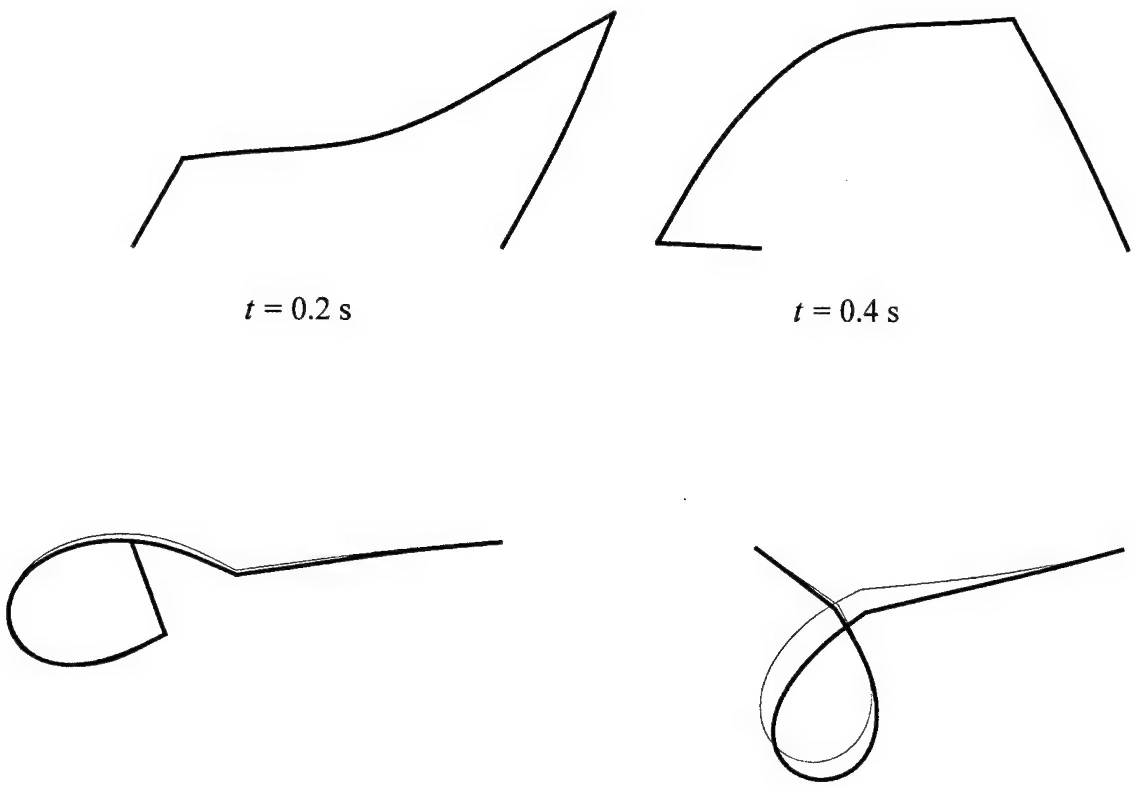

Fig. 8 panels: $t = 0.2$ s, $t = 0.4$ s, $t = 0.6$ s, $t = 0.8$ s

Fig. 8. Large deformations of the four-bar mechanism
— Model 3 with pinned frame
— Model 3 with tangent frame

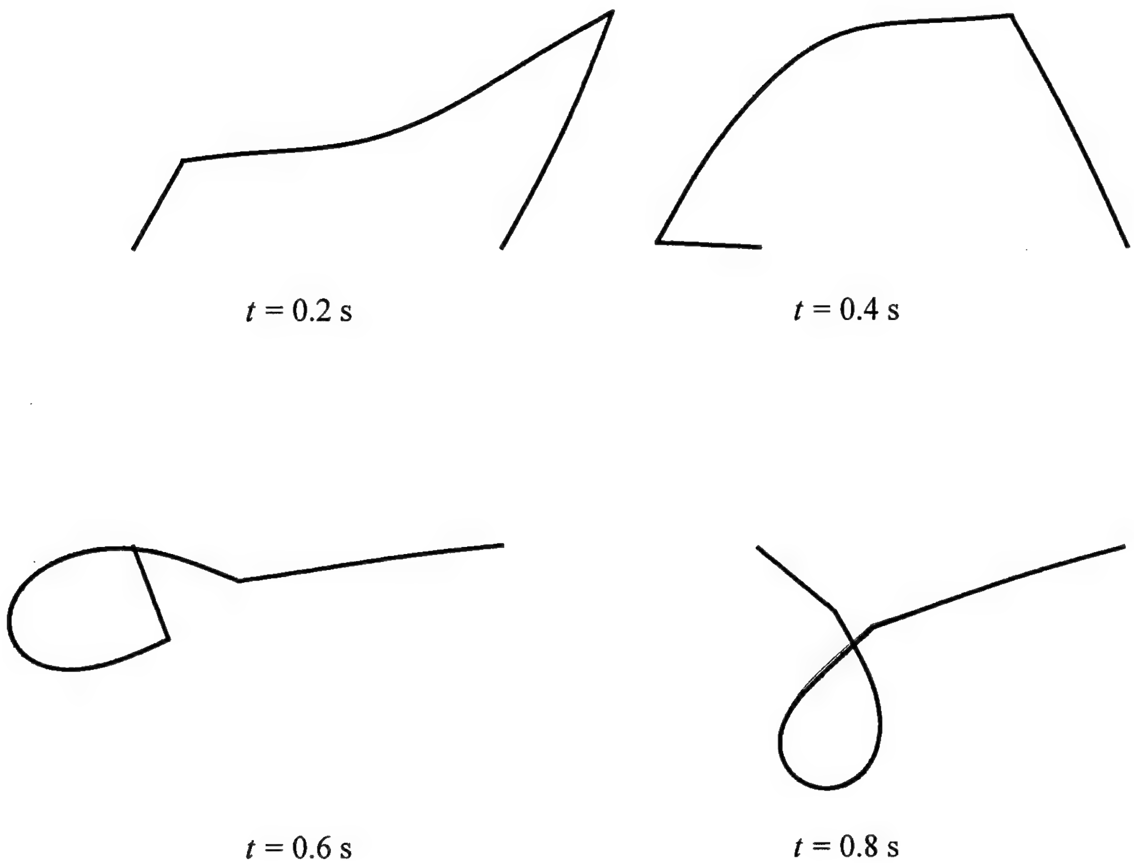

Fig. 9. Large deformations of the four-bar mechanism
— Model 4 with pinned frame
— Model 4 with tangent frame

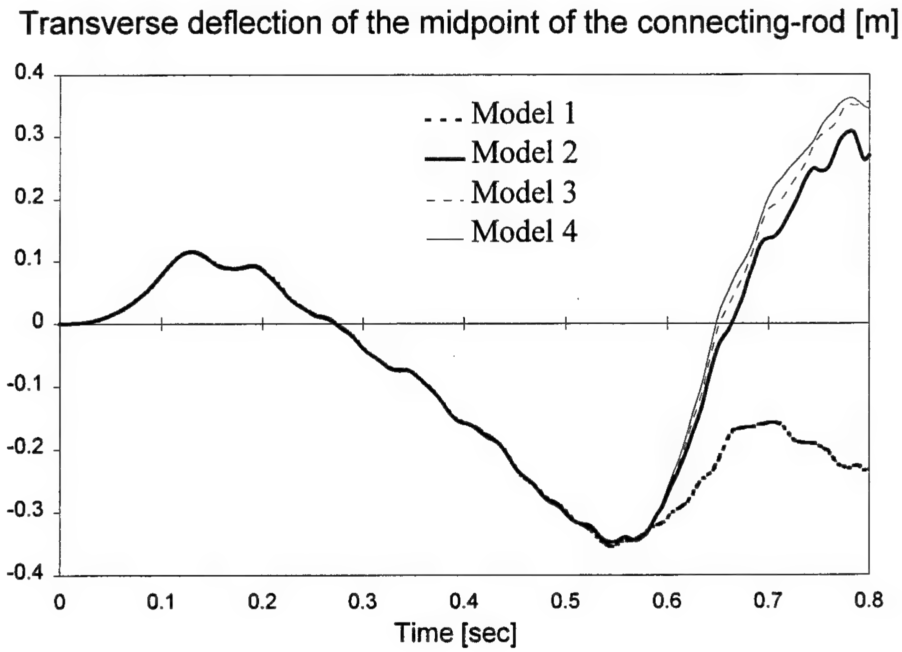

***a*)** Pinned frame

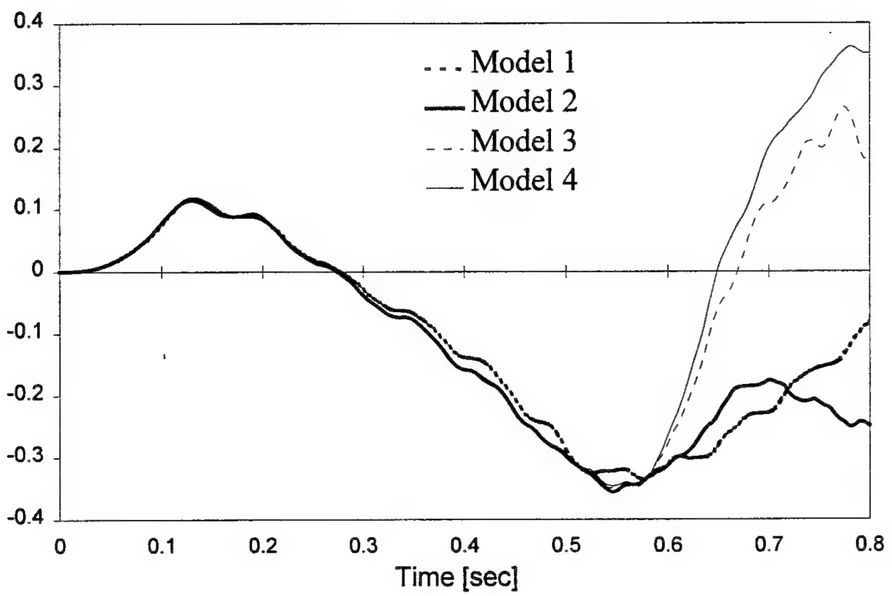

***b*)** Tangent frame

Fig. 10. Transverse deformation of the midpoint of the connecting-rod using different models

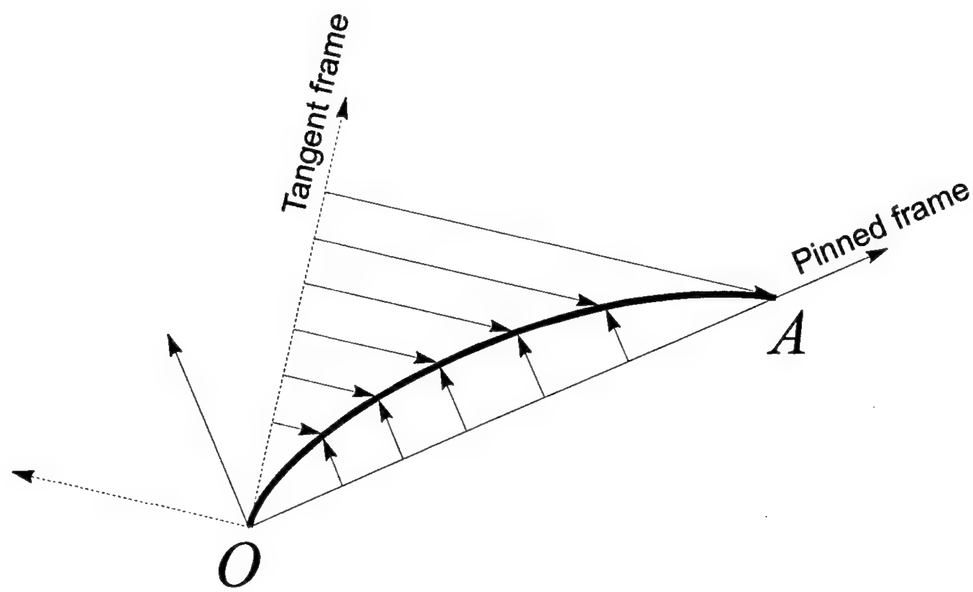

Fig. 11. Transverse deflections measured by the tangent system and by the pinned system

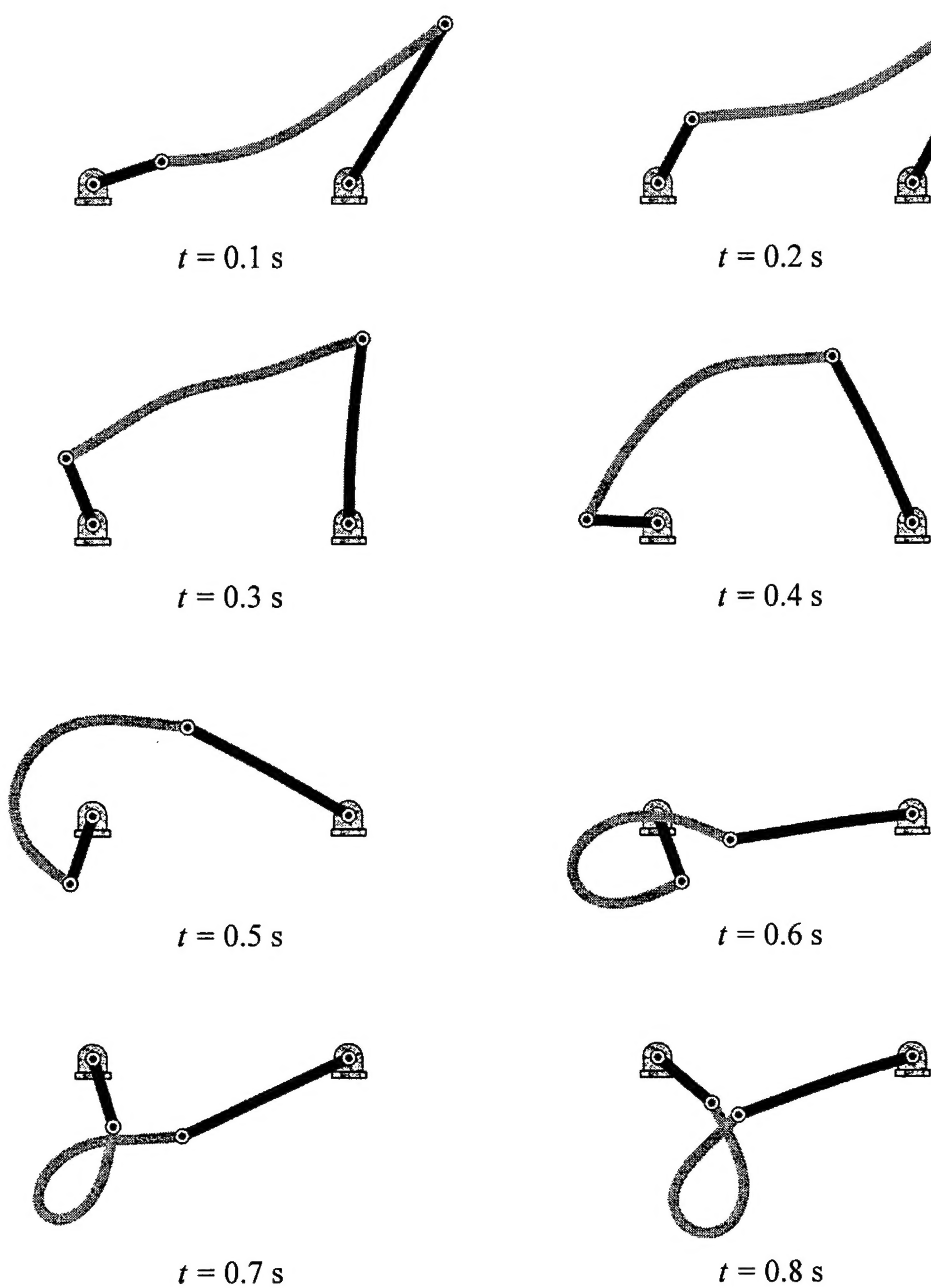

Fig. 12. Computer animation of the motion of the four-bar mechanism

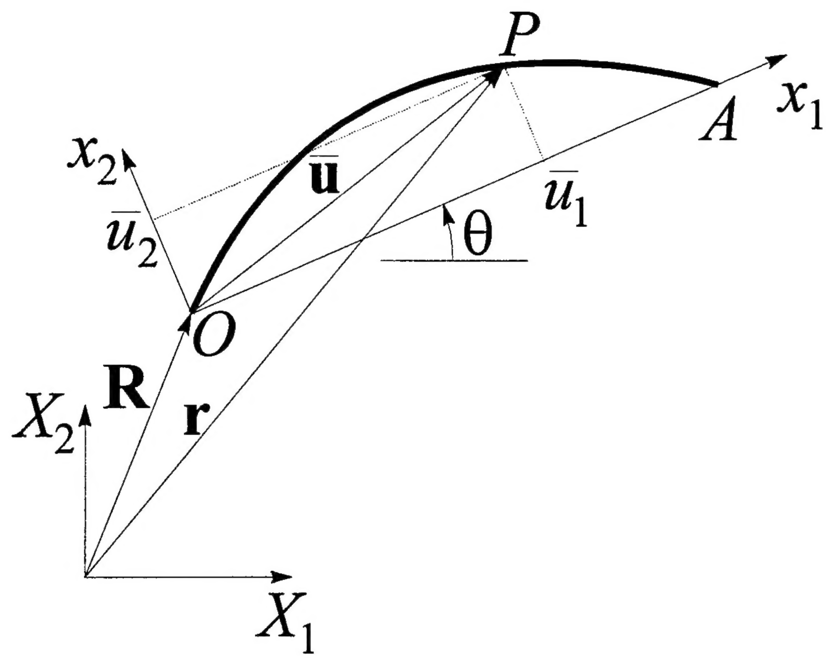

Fig. 13. Floating frame of reference formulation

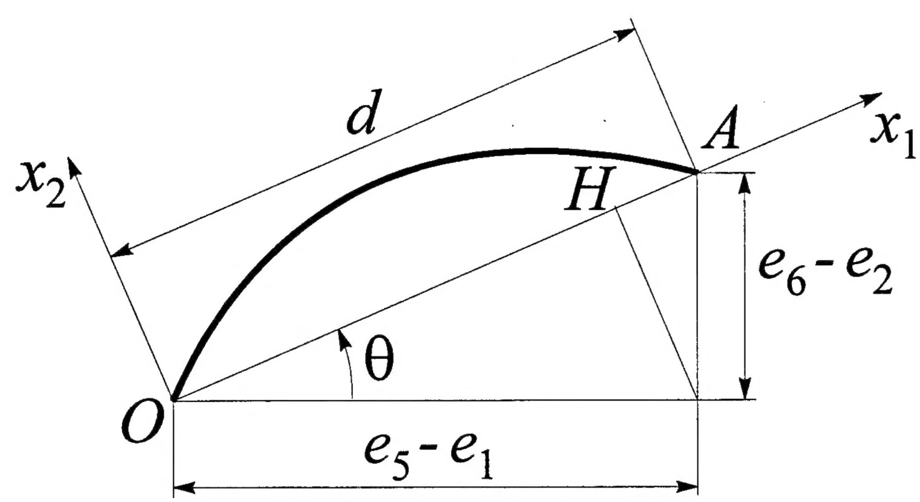

Fig. 14. Relationship between the coordinates of the two formulations

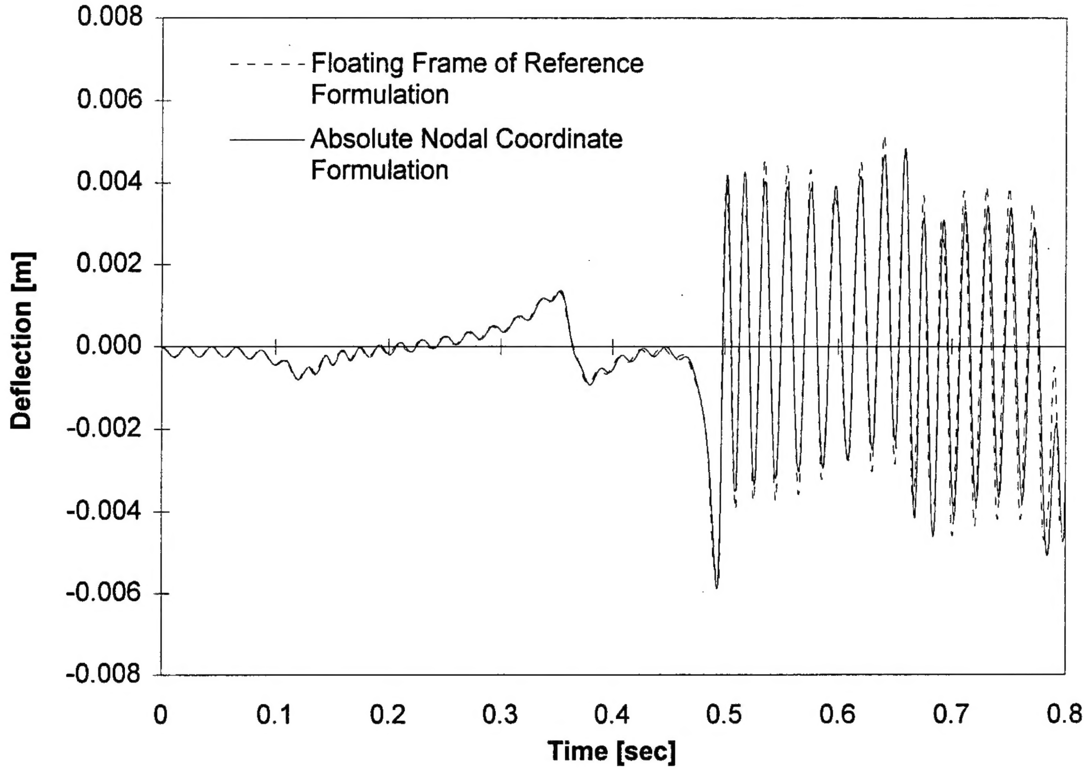

Fig. 15. Comparison between the results of two different formulations

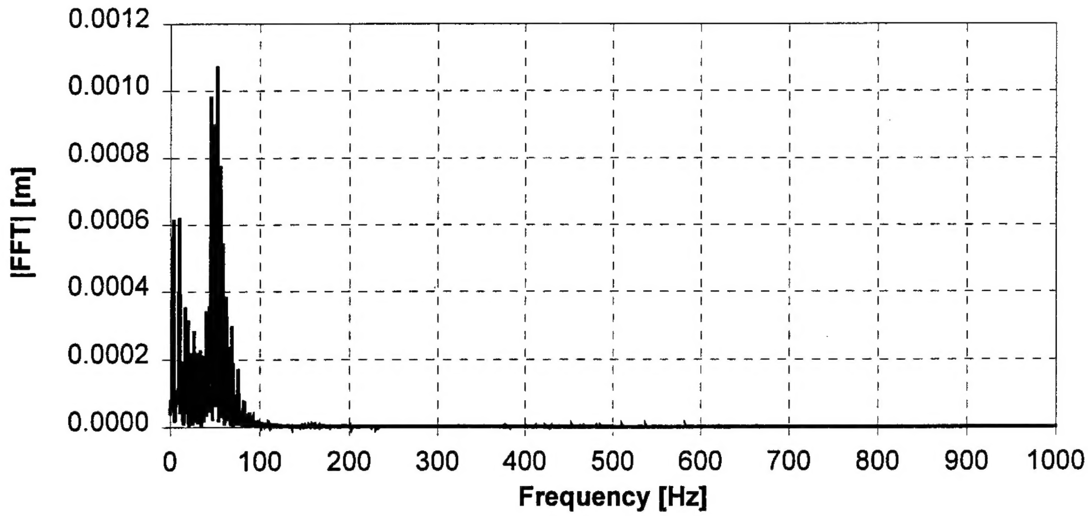

a) Large frequency window

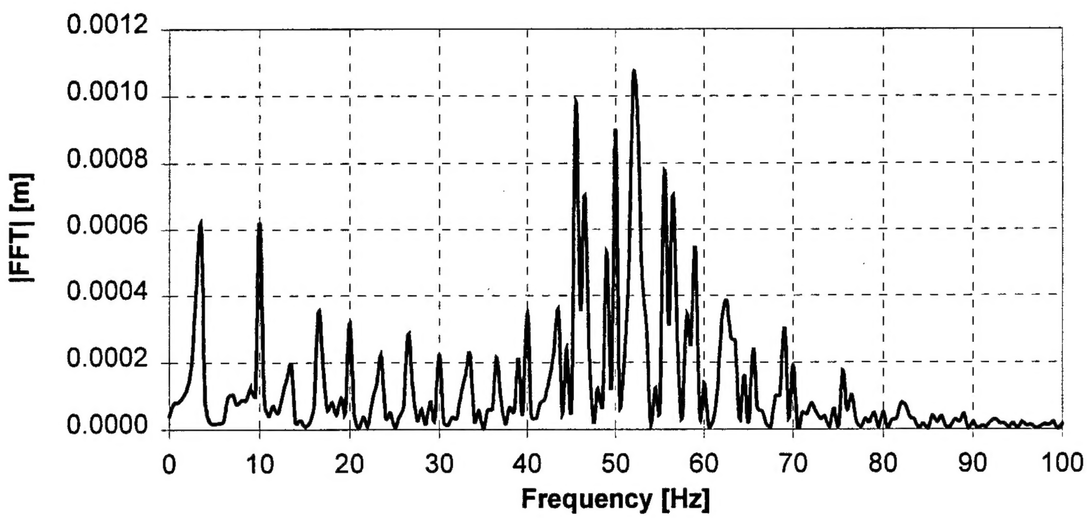

b) Small frequency window

Fig. 16. FFT of the midpoint deflection of the connecting rod